A FRACTIONAL ORDER DYNAMICAL SYSTEM AND SIMULATION WITH AN APPLICATION ON INFECTIOUS DISEASES

RUYA IMAD JAMAL JAMAL

AUGUST 2025

ÇANKAYA UNIVERSITY

GRADUATE SCHOOL

MATHEMATICS DEPARTMENT
MATHEMATIC MASTER'S THESIS

A FRACTIONAL ORDER DYNAMICAL SYSTEM AND SIMULATION WITH AN APPLICATION ON INFECTIOUS DISEASES

RUYA IMAD JAMAL JAMAL

AUGUST 2025

ABSTRACT

A FRACTIONAL ORDER DYNAMICAL SYSTEM AND SIMULATION WITH AN APPLICATION ON INFECTIOUS DISEASES

JAMAL, RUYA IMAD JAMAL
MATHEMATICS MASTER'S THESIS

Supervisor: Assist. Prof. Dr. Erkan Murat TÜRKAN
Co-Supervisor: Dr. Nurgül GÖKGÖZ KÜÇÜKSAKALLI
August 2025, 106 Pages

Fractional calculus provides a powerful mathematical framework that extends classical calculus to capture memory and hereditary properties in dynamic systems. Its application to epidemiology offers deeper insights into the complex dynamics of infectious disease transmission.

This study focuses on compartmental epidemic models, beginning with the classical SIR model, which divides the population into Susceptible (S), Infected (I), and Recovered (R) groups. Extensions of this framework include the SEIR model, which accounts for an Exposed (E) class, the SIS model, which allows recovered individuals to return to susceptibility, and the Carrier model, which introduces asymptomatic or persistent carriers. A more generalized model, the SEIQRV, divides the population into six compartments: Susceptible (S), Exposed (E), Infected (I), Quarantined (Q), Recovered (R), and Vaccinated (V).

The basic reproduction number R_0 serves as a fundamental threshold metric for assessing disease spread, with stability analysis conducted through equilibrium points and the Jacobian matrix. The system's stability depends on the eigenvalues of the Jacobian, which determine whether the disease-free or endemic equilibrium is attained. Numerical simulations, performed in MATLAB, examine the SEIQRV model under fractional-order derivatives with different orders (α=1,0.9,0.8). The

results demonstrate that incorporating quarantine and vaccination compartments effectively lowers the reproduction number, thereby controlling the spread of infection.

Overall, the study highlights the importance of fractional-order epidemic models in evaluating intervention strategies and emphasizes their role in public health planning and disease management.

Keywords: Fractional calculus stability , Numerical analysis , mathematical modeling, Basic reproduction Numbers, epidemic, spread disease, Stability analysis.

ÖZET

KESİRLİ DERECELİ DİNAMİK SİSTEM VE BULAŞICI HASTALIKLAR ÜZERİNE BİR UYGULAMA İLE SİMÜLASYON

JAMAL, RUYA IMAD JAMAL
MATEMATİK YÜKSEK LİSANS TEZİ

Danışman: Dr. Öğr. Üyesi Erkan Murat TÜRKAN
Ortak Danışman: Dr. Nurgül GÖKGÖZ KÜÇÜKSAKALLI
Ağustos 2025, 106 Sayfa

Kesirli kalkülüs, klasik kalkülüsü genişleten ve dinamik sistemlerde bellek ve kalıtım özelliklerini yakalamaya imkân tanıyan güçlü bir matematiksel çerçeve sunar. Epidemiyolojiye uygulanması, bulaşıcı hastalıkların karmaşık yayılım dinamiklerini daha derinlemesine anlamaya olanak sağlar. Bu çalışma, klasik SIR modeliyle başlayan bölmeli epidemik modelleri ele almaktadır. SIR modeli, toplumu Duyarlı (S), Enfekte (I) ve İyileşmiş (R) gruplarına ayırır. Bu yapının genişletilmiş halleri arasında maruz kalan bireyleri dikkate alan SEIR modeli, iyileşen bireylerin yeniden duyarlı hale gelebildiği SIS modeli ve asemptomatik ya da kalıcı taşıyıcıların dâhil edildiği Taşıyıcı modeli bulunmaktadır. Daha genel bir yapı olan SEIQRV modeli ise nüfusu altı bölmeye ayırmaktadır: Duyarlı (S), Maruz (E), Enfekte (I), Karantinada (Q), İyileşmiş (R) ve Aşılı (V).

Temel üreme sayısı (R_0), hastalığın yayılımını değerlendirmede kritik bir eşik ölçütü olarak kullanılır. Denge noktaları ve Jacobian matrisi üzerinden yapılan kararlılık analizi, sistemin hastalıksız veya endemik dengeye ulaşıp ulaşmayacağını belirler. MATLAB ortamında gerçekleştirilen sayısal benzetimler, farklı kesirli türev dereceleri (α=1,0.9,0.8) altında SEIQRV modelini incelemektedir. Sonuçlar, karantina ve aşılama bölmelerinin eklenmesinin üreme sayısını düşürerek enfeksiyonun yayılımını kontrol etmede etkili olduğunu göstermektedir.

Genel olarak, bu çalışma kesirli türevli epidemik modellerin müdahale stratejilerinin değerlendirilmesinde önemini vurgulamakta ve bunların halk sağlığı planlaması ile hastalık yönetimindeki rolünü öne çıkarmaktadır.

Anahtar Kelimeler: Kesirli hesaplama kararlılığı, Sayısal analiz, Matematiksel modelleme, Temel üreme sayıları, salgın, hastalık yayılımı, Kararlılık analizi.

ACKNOWLEDGEMENT

First and foremost, I would like to thank my supervisor Dr.NURGÜL GÖKGÖZ KÜÇÜKSAKALLI for guiding and helping me along the way in writing this research. Discussing my progress, problems, and ideas with my Supervisor Dr.NURGÜL GÖKGÖZ KÜÇÜKSAKALLI helped me tremendously in understanding the logic behind the research. It made me better realise the technical need for this research work. Without his time and help, none of this research would have been possible, and I am grateful to her for giving me the opportunity to work on this interesting subject. I am also very thankful to my family, who always supported me through the whole of this journey.

TABLE OF CONTENTS

LIST OF TABLE

LIST OF FIGURES

CHAPTER I
INTRODUCTION

Fractional calculus is an advanced mathematical method that goes beyond traditional calculus to include real differential and integral powers (Singh, 2022). Unlike traditional calculus, which relies on integer arrangements, fractional calculus explores integrals and derivatives of every real and realistic arrangement, which contributes to providing a flexible framework for modeling systems with memory and genetic properties (Inoue 2021). This flexibility has led to its widespread use in many scientific fields, other than biology, where fractional calculus is useful and useful, especially in explaining and interpreting phenomena affected by long-term memory effects. Biological processes are often characterized by difficult dynamics and are based on past and present states, and partial control systems are optimized to overcome these difficulties and complexities (Wu 2023). By exploiting dynamical systems of fractional order, researchers can accurately model processes such as large and abnormal cell outbreaks, population dynamics, and ecosystem interactions, which improves our understanding of these difficult biological systems (Gao 2024).

In recent years, fractional calculus has become an important tool in the modeling of diverse phenomena in various disciplines, providing a powerful alternative to traditional calculus by extending its scope to include non-integer orders (Oldham and Spanier 1974). This mathematical framework is known as fractional calculus, and it differs from classical calculus in that it allows the use of operators capable of handling powers of real numbers, leading to integrals and derivatives of any fractional order. The concept of fractional calculus, which has its origins in the important fundamental research of Liouville and Riemann in the 19th century, has been developed to become an effective approach to modeling systems with memory and genetic properties—features that are important for many applications in biology, engineering, and physics (Podlubny 1999).

Applied mathematics is witnessing significant progress in explaining natural events and also biological or environmental systems, where the use of the Fractional

Order Dynamical Systems is considered one of the most important advanced methods that provide greater knowledge of the method of the difficult environmental system (Dorčák 2013). Where the usual mathematical examples with a precise order are sometimes few in explaining the correct and sometimes different environmental interactions, and according to the fact that many environmental events are characterized by opposite and uncertain features, and change with many contemporary fluctuations (Merlin 1949). Here the necessity of the fractional order appears, which facilitates the explanation of more severe dynamics of these events through a better explanation of the correct fluctuations over time. Where the Fractional Order Dynamical Systems gains from mathematical operations that have an imprecise position, which allows for the increase of modern aspects through the process of researching the effectiveness of time and external and internal interactions within the environmental system, such as active chemical interactions, the progress of epidemics, the interaction of the biological system, and the movement of neural signs (Thirring 2013). Despite the necessity of such research, the environmental procedures of the fractional system are still in their early stages, as many studies need adequate examples to investigate difficult environmental events with correct mathematical methods.

Unlike conventional models, fractional order models are non-local, meaning that the current state of the system is based not only on current conditions and circumstances, but also on its entire historical trajectory. This property makes fractional calculus particularly useful in modeling difficult biological systems. Biologically difficult behaviours often depend on past events or stimuli. For example, in the field of systems biology, it has been used to characterize the dynamics of cell signalling and tissue proliferation, both of which exhibit unusual phenomena of non-classical diffusion and relaxation (Maggin 2006). These memory effects are important in biological systems, where responses to stimuli or the release of important chemical signals are influenced by past states, leading to more accurate and detailed models than those based on integer differential equations (Metzler and Clafter 2000).

One application of the main task of fractional calculus is to exploit fractional partial differential equations (FPDEs), which allow the modeling of distributed temporal and spatial phenomena with natural memory effects. They are particularly used in dynamic systems with fractional order in biology. Biodiversity uses these values and principles to capture the difficult behaviors observed in populations, such as population distribution, competition for resources, and interactions between species.

This is very important in the field of epidemiology and ecology, where more accurate models are important and necessary to predict population growth, species survival, and epidemic outbreaks (Dethelm 2010; Sun et al. 2011).

Studies and research can aim to ensure that fractional-order models provide the best fit to ecological data compared to traditional integer-order models because they have the ability and potential to mix long-range dependencies and non-local interactions (Ahmed et al. 2007).

In the field of biological modeling, time-fractional differential equations, in which the order of the time derivative is a fraction rather than an integer, are widely used to describe processes that have memory for genetic properties. Such models have been implemented to simulate sub- and super-spreading, i.e., these phenomena are widespread in biological tissues where particle motion is limited by structural heterogeneity, such as cell membranes and extracellular matrices (Benson et al. 2000; Anastasio 1994). For example, in the field of cell biology, standard diffusion equations cannot adequately capture the motion of particles in crowded environments. Instead, fractal models provide a more accurate representation by accounting for abnormal diffusion patterns, improving our perception and understanding of cellular processes (Gorenflo et al. 2002; Hatef and Yousefi 2013). Fractional order is also an important tool for understanding population dynamics in ecosystems where memory effects are important, such as in resource competition and predator–prey interactions. In this context, fractional and integral quotations are an effective way to integrate historical data, which reflects the influence of past interactions on future population states (Tarasov 2011; Elsayed and Elsaidi 2014). For example, the two-dimensional fractional population model takes into account past and current population levels and introduces a lag factor that better models global environmental interactions.

Indeed, these models exhibit oscillatory behavior and difficult stability conditions that are more consistent with results for natural ecosystems than traditional models (Kexue and Ding 2013). In addition, improvements in the calculations related to the treatment of FPDE derivatives have led to the expansion of the use of fractional calculation in biological modeling. Numerical methods, such as the Chebyshev spectral method, have proven their effectiveness in discretizing fractional derivatives and dealing with non-local properties of fractional order equations, especially in two-dimensional models (Chen et al. 2014; Agrawal 2002).

Chebyshev's spectral method relies on orthogonal bounds to achieve accurate approximation of solutions, making it superior to conventional finite difference methods in handling the computational complexity of FPDE equations (Ortigueira 2006; Atangana and Baleanu 2016).

Hence, this research seeks to explain the fractional order Dynamical Systems For Biological Phenomena and close a necessary cognitive and interpretive gap, by providing examples of fractional environmental events, and explaining their expected effectiveness and realistic procedures by addressing necessary vital topics. Fractional order biological system. SIR model

$$S(0) = 990;\ I(0) = 10; R(0) = 0;\ \beta = 0.3;\ \gamma = 0.1; \quad R_0 = \frac{\beta}{\gamma} = \frac{0.3}{0.1} \quad (1.1)$$

1.1 PROBLEM STATEMENT

The progress of environmental events and their response to biological and contemporary elements poses a huge difficulty for scientists. It is difficult to use the usual mathematical examples to explain the difficult aspects of contemporary transformations within the behaviour of living creatures and their communication with each other. The difficulty appears greater when the situation is related to the research of environmental phenomena that require a correct explanation of the movement of parts, the spread of epidemics, and nervous transmission. The dynamic system with a precise status neglects a number of necessary trends that are specific to the environmental system, such as the memory effect and the transformations of the wheel and response over time. Therefore, the lack of adequate examples that focus on the system with a fractional status in explaining environmental phenomena leads to a lack of access to correct and complete knowledge of its dynamics, which reduces the ability of scientists to provide realistic treatments for difficult biological and health crises.

Contemporary research requires adequate knowledge by investing in the fractional system to analyse these events, which requires the implementation of studies that participate in closing this deficit, thus opening the field towards modern procedures that benefit society and science. Traditional mathematical models of biological systems, which rely on the calculation of correct order, often fail to capture the full complexity of biological phenomena that include memory and genetic properties.

For example, traditional outbreak models may fail to explain how particles move through cellular environments or how epidemics spread through communities, where interactions are influenced by historical conditions. This limitation limits our ability to accurately predict, simulate, and control biological processes. Fractal models, which allow for non-local dynamics and are based on history, have shown promise in improving these gaps. However, there are still problems and difficulties in developing efficient numerical methods to solve fractal models, especially in high-dimensional contexts that more accurately reflect real-world biological phenomena.

1.2 OBJECTIVES

The main purpose of this research is to improve and validate the accuracy and validity of the Fractional Order Dynamical Systems for Biological Phenomena. This research shows:

1- Develop a two-dimensional biological population model with a fractional order that takes into account memory and genetic characteristics, providing a more accurate representation of environmental interactions.

2- Apply numerical methods such as the L1 scheme for fractional time derivatives and Chebyshev spectral methods for spatial derivatives, to process the fractal model with quality and efficiency.

3- Interpret and evaluate the performance quality of the developed model to accurately capture biological phenomena, excluding unusual cell explosions and population interactions influenced by historical conditions.

4- Demonstrate the benefits of fractal order models compared to traditional integer models for simulating biological dynamics involving complex boundary conditions and long-term memory effects.

1.3 RESEARCH STRUCTURE

1. Introduction: This section provides a comprehensive overview of fractional calculus and its importance for biological modeling, with a focus on the limitations of traditional integer-order models.

2. Literature Review: Previous studies on the applications of fractional orders in biology are reviewed, highlighting population dynamics, the role of memory in biological systems, and anomalous diffusion.

3. Methodology: Model Formulation: A fractional-order biological population model is illustrated, explaining how fractional derivatives can be used to combine memory effects in two-dimensional systems. Numerical Methods: The numerical methods used are reviewed, including the L1 method for time fractional derivatives and the Chebyshev spectrum methods for spatial derivatives, as well as error analysis, interpretation, and convergence measures.

4. Results and Discussion: Simulation and Analysis: Operations are performed to test the performance of the model, and demonstrate its efficiency in capturing challenging biological dynamics. Comparisons with integer-degree models are made to highlight the benefits of fractional methods. Discussion: Interpret the results and insights derived from the use of fractal models, highlighting practical applications in the fields of ecology, biology, and epidemiological modeling.

5. Conclusion and future work: Provide a summary of the results with suggestions for further research, particularly in the process of extending the scope of fractal methods to include more difficult and complex biological systems.

This will assist research in mathematical modeling of biological systems by establishing a fractal-based framework that captures key memory and genetic factors that are often neglected by traditional models. This result will contribute to enhancing the ability and potential to simulate and predict difficult biological dynamics, providing insights that may be useful in environmental conservation efforts, ecosystem management, and public health interventions.

CHAPTER II
LITERATURE REVIEW

2.1 INTRODUCTION

This chapter presents a collection of published literature on the subject and a theoretical framework for understanding how to implement fractional order dynamical systems (FODS) on biological phenomena based on combining mathematical meaning with the inherent difficulty of biological systems. Fractional Order (FO), which augments ordinary differential calculus to include integrals and derivatives of imprecise order, provides a powerful mathematical approach to modeling the difficult dynamics of biological systems. This framework is based on many of the basic principles and ideas of the study as discussed in the scientific literature.

2.1.1 Fractional-Order Dynamical Systems

2.1.1.1 Fractional Order Derivatives Integral Definition

In the domains of dynamical systems and control theory, a fractional-order system refers to a system described by a fractional differential equation involving derivatives of non-integer order (Monje 2010). These systems exhibit what is known as fractional dynamics. Fractional derivatives and integrals are utilized to model phenomena in a power-law nonlocality, long-range dependence governed by power-law behavior, or fractal-like properties (Cattani and Carlo 2015: 31). Such systems have proven valuable in analyzing the anomalous behaviors observed in various fields, including physics, electrochemistry, biology, viscoelastic materials, and chaotic systems (Monje 2010). A fractional-order dynamical system can generally be expressed in the following form:

$$H(D^{\alpha_1,\alpha_2,\ldots,\alpha_m})(y_1, y_2, \ldots, y_l) = G\left(D^{\beta_1,\beta_2,\ldots,\beta_n}\right)(u_1, u_2, \ldots, u_k) \qquad (2.1)$$

In a general fractional-order dynamical system, H and G represent functions of the fractional derivative operator D with orders α1, α2,…,αm and β1,β2,…,βn and yi and uj are time-dependent functions representing the system's output and input. A commonly studied special case is the linear time-invariant (LTI) system with a single

variable, which simplifies the general formulation and has practical applications in various fields:

$$\left(\sum_{k=0}^{m} a_k D^{\alpha_k}\right) y(t) = \left(\sum_{k=0}^{n} b_k D^{\beta_k}\right) u(t) \tag{2.2}$$

The orders αk and βk in fractional-order systems are generally complex, but two notable cases arise. First, when the orders are commensurate, they can be expressed as:

$$\alpha_k, \beta_k = k\delta, \;\; \delta \in R^+ \tag{2.3}$$

Second, when the orders are rational, they are given as:

$$\alpha_k, \beta_k = k\delta, \;\; \delta = \frac{1}{q}, q \in Z^+ \tag{2.4}$$

In the special case where q=1, the derivatives reduce to integer orders, and the system becomes an ordinary differential equation. Consequently, LTI systems can be classified progressively by their order: general, commensurate, rational, or integer.

2.1.1.2 Analysis for Fractional Differential Equations

There is two ways of fractional differential equations which are:

- **Existence and uniqueness**: For a fractional-order initial value problem, under the assumption of the continuity of the function f, the given differential equation can be transformed into an equivalent integral equation:

$${}_0^C D_t^{\alpha} x(t) = f\big(t, x(t)\big), \;\; t \in [0, T], \;\; x(0) = x_0, \;\; 0 < \alpha < 1 \tag{2.5}$$

A solution space can then be constructed, and using this integral equation, a continuous self-map can be defined over the solution space. By applying a fixed-point theorem, a fixed point can be obtained, which serves as the solution to the original equation.

- **Numerical Simulation:** (Diethelm 2006) stated that to numerically simulate the solution of these equations, Kai Diethelm proposed using the fractional linear multistep Adams–Bashforth method or quadrature methods. These approaches are widely recognized for their effectiveness in solving fractional-order systems.

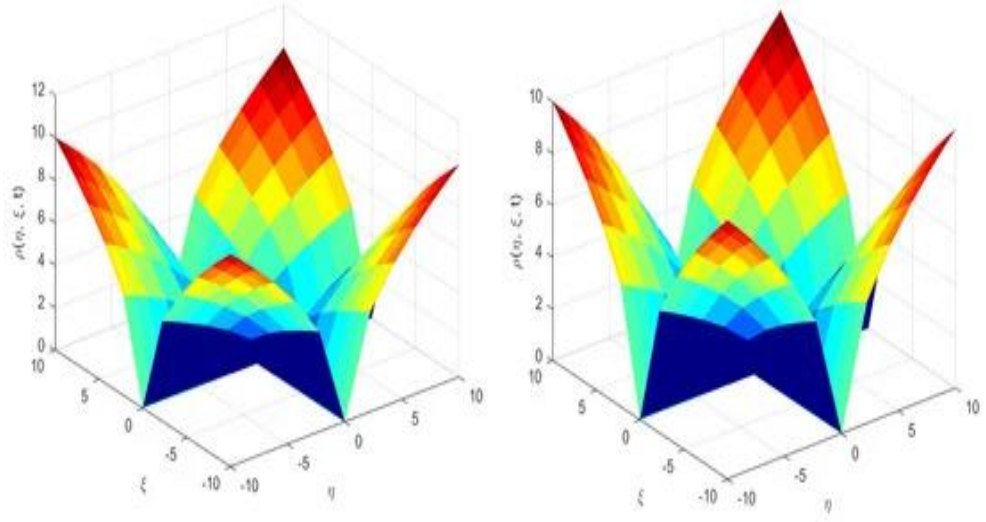

Figure 1: Example 1 _ Comparisdfgon of the exact solution (left) and the numerical solution (right) with N=15 collocation points.

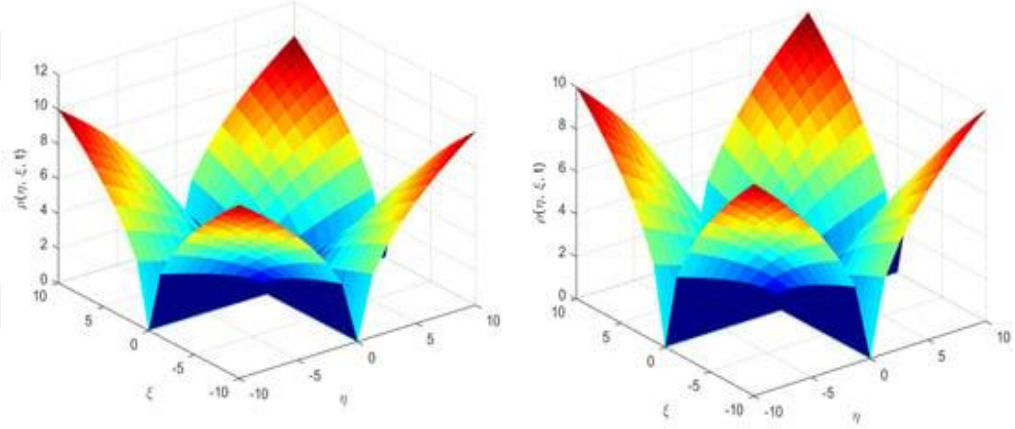

Figure 2: Example 1 _ Comparison of the exact solution (left) and the numerical solution (right) with N=50 collocation points.

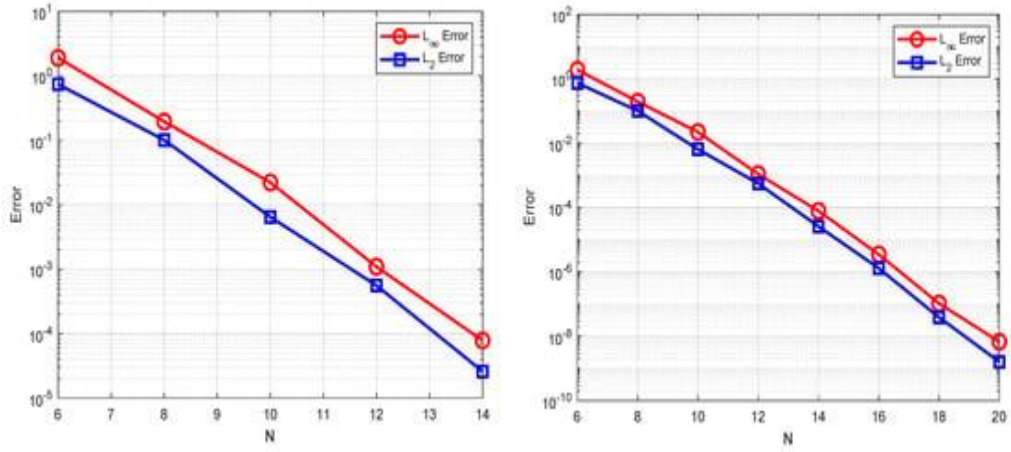

Figure 3: Example 1_ Error analysis between the exact solution and the numerical solution at N=15 (left) and at N=20 (right).

2.1.1.3 Foundations of Fractional-Order systems

One of the main approaches within fractional order systems is that fractional order integrals/derivatives affect the properties of dynamical systems when combined within them. So the interpretation of the main features of the method is one of the main focuses within that framework. A number of selected contributions within that context are described below, starting with stability issues. In the context of regular time, the first easy test of stability was made by (Matignon 1998: 145–158). The result is provided for stable conformal systems of the same order, and stability is tested based on proofs of zeros in a variety of different directions (often called poles or poles). Through this test, the fractional order method leads to a left-handed change from a hard quantity to the same order quantity. Many studies have been designed based on this principle, with the focus on non-conformal and time-shifting systems. Matignon's summation has also been extended to include systems with fractional derivatives of relative order (Petrá˘s 2009: 269–298). An additional approach within this framework has been presented by (Busłowicz 2008: 319–324).

This statement discusses the interpretation of stability for a specific set of time-delayed systems. It shows that a number of stability summations established for classical (fine-order) systems from the direction of the Mykhailov stability level can be used effectively for the set of systems with fractional orders. This approach has been recently continued in (Mendiola-Fuentes 2018: 2779–2790) which extends Matignon's hypothesis to include systems with identical orders. In addition, the tasks accomplished on large scales illustrate the meaning of the interpretation of stability.

Such rule-based methods as Nyquist stability have been established with excellence for systems with identical and non-identical fractional orders as well as in non-identical and non-identical situations (Tavazoei 2020). The researcher of that section says that many of the difficulties of stability present within systems of fractional and fine orders can be resolved using the Mikhailov pattern. However, while explaining the stability of systems of non-identical orders, Lyapunov methods are generally used (Li 2010: 1810–1821), although they are more complicated during application compared to methods such as Nyquist or Mikhailov.

In accordance with the methods described above, the stability update of systems of fractional orders during the time difference occurred. The first result of stability in that context was designed by D. Zielinski and Sir Wisock within the source (Dzieli´nski 2008: 1543–1556). It provides necessary suggestions for stability within

the statement of the method of setting the same fractional order during the time difference using the moving forward Greenwald-Letnikov divergence. It is based on the poles of the different directional manifold shown within the Z range.

These necessary suggestions for stability remain and need to be developed, so a pattern based on poles was discovered. For this reason, matching stability proposals (Busłowicz 2013: 779–786) have been designed based on so-called stability locations. Also, within reference, interpretationally designed proposals have been designed for this group of systems. It is seen that during the time-sparse modes, stability proposals are based on the explanation of the fractional difference. Within the relevant Greenwald-Letnikov backward fractional groups (usually understood in the sense of Nabla groups), there is an additional stability proposal. The stability locations such as the poles for this group of systems are updated independently within the sources (Ostalczyk 2016). Analogous to the stability sum of the delta (forward-moving) and Nabla (backward) groups, it is clear that the meaning of the group operator affects the stability of the method. Also, during the time-sparse mode, the operator used within the fragmentation task affects the stability of the emerging sparse method. As for the three most widely used operators in the Euler, Tusten and Alawi modes, this situation has been demonstrated in the source (Stanisławski 2018: 1–9).

Also, stability suggestions are gained for discrete-time systems using the Caputo explanation and also for non-stationary order modes (Mozyrska 2018: 1–4). As in the discrete-time mode, the stability explanation for systems with non-identical orders is more competitive than for systems with identical orders. Within this framework, it is possible to discover a number of data that include interpretive results that are difficult to achieve (see Wyrwas 2013: 167–171). However, it has been confirmed that the Mikhailov model of stability works on easy stability suggestions for systems with non-identical orders under Naples groups. As in the constant-time setting, in many publications a variety of systems with discrete fractional orders have been examined in the setting of time-delayed systems, continuous systems, time-shifted systems and others. Also, the interpretation of the stability of non-identical systems within discrete time is more competitive, and many results within this setting are based on Lyapunov stability (Antoulas 2005).

2.1.1.4 Control Theory of Fractional-Order Systems

According to (Zhao 2021), the discrete fractional Fourier transform (DFRFT) is discussed, with multiple definitions proposed for this transform. The most notable of these is the multiweighted fractional Fourier transform (M-WFRFT). However, proving the unitarity of the M-WFRFT presents a significant challenge. To address this difficulty, Zhao employs several basic functions, including the weighted-type fractional Fourier transform, the fractional-order matrix, and the eigendecomposition-type fractional Fourier transform, to analyze and describe the unitarity of the M-WFRFT. It was observed that the M-WFRFT includes only four effective weighting terms, which contradicts its original definition, which anticipated the inclusion of many more terms. This discrepancy suggests that the M-WFRFT does not fully adhere to the broad scope of its definition. Additionally, Zhao reviewed previous work published in (Digit Signal Process 2020: 104: 18), which sought to verify the unitarity of the M-WFRFT using MATLAB. Upon examination, Zhao found that the MATLAB program code used in the prior research contained inaccuracies, raising concerns about the validity of the unitarity verification results.

According to (Muresan 2022) there is a significant focus on the growing body of research surrounding fractional-order controllers, especially fractional-order PID controllers. These controllers are a variation of the conventional PID (Proportional-Integral-Derivative) controllers, incorporating fractional orders instead of integer ones, which can offer more flexibility in system control. Over time, these controllers have been proposed in various configurations, each offering unique approaches for tuning and implementing them. Despite the promising potential of fractional-order PID controllers, their adoption in industrial applications has not yet become widespread. This could be due to the complexity involved in tuning and implementing these controllers effectively. To address this challenge, recent research has explored the integration of auto-tuning methods, which would automate the process of adjusting the controller's parameters, making them more accessible for industrial use. Muresan’s work reviews several existing auto-tuning approaches for fractional-order PID controllers, with a focus on the most recent developments in the field. The study also compares different auto-tuning algorithms and their applicability to various industrial processes. Numerical examples are provided to demonstrate the practical use of these algorithms, highlighting their potential to improve the performance and ease of use of fractional-order controllers, especially in simpler industrial tasks.

(Khan 2022) the authors propose an interval estimator designed for a fourth-order nonlinear SEIR (susceptible–exposed–infected–recovered) model. This model is used to track the spread of infectious diseases, which, according to the World Health Organization (WHO), are among the leading causes of death worldwide. Effective monitoring of these diseases is crucial for developing strategies to intervene and reduce their spread. The study focuses on a practical scenario where some factors involved in the SEIR model are uncertain.

The **SIR model** is one of the easiest models to understand, and many other models are based on it (Harko 2014: 184–194). The model has three parts:

- **S**: The number of people who are likely to get sick. When a person who can get sick gets close to someone who is sick, the healthy person catches the disease and becomes sick too.
- **I**: The count of people who are sick. These are people who have the infection and can pass it on to others who are not infected.
- **R** is for the number of people who have been removed (and are immune) or have died. These are people who got sick, have either gotten better and are no longer sick, or have died. It is thought that the number of deaths is very small compared to the total population.

This section can also be called "recovered" or "resistant". " This model can predict well for infectious diseases that spread from person to person and where getting better gives lasting protection, like measles, mumps, and rubella (Yang 2020).

Specifically, there are disturbances in the model, and certain variables like input measurements, output measurements, and the transmission rate from susceptible to exposed individuals are imprecise. However, these uncertain factors fall within known intervals, which presents a challenge for accurately predicting the disease's progression. To address these challenges, Khan and the team introduce an interval estimator. This estimator uses an observability matrix, a mathematical tool that helps estimate the true states of a system despite uncertainties. The key advantage of this method is that it produces a guaranteed range (or interval) for the true states of the SEIR model without requiring the computation of an "observer gain," a parameter typically needed in other estimation methods. By removing this dependency, the proposed approach offers greater flexibility. The study also examines the behavior of the estimated states over time, specifically the convergence of the estimated interval width. Over a finite period, the interval width of the estimated state vector is shown to converge to a known value, ensuring that the estimation error stabilizes. This provides

a level of confidence that the interval estimator will eventually provide a reliable estimate of the system's true states.

Finally, the authors validate their method through simulations, which demonstrate the effectiveness and reliability of their approach in estimating the true states of the SEIR model even under conditions of uncertainty and noise.

(Makhlouf 2022) a new approach is introduced to establish finite-time stability (FTS) for neutral fractional-order systems with time delays (NFOTSs). These systems are characterized by their fractional-order derivatives, which account for memory effects, and they also include time delays, adding complexity to their behavior. The concept of finite-time stability refers to the system's ability to reach a stable state within a finite amount of time, which is a key aspect for ensuring the system's reliability in real-world applications. Makhlouf builds upon the well-known Gronwall inequality, a mathematical tool often used in stability analysis, to show that the NFOTSs are finite-time stable. The Gronwall inequality provides bounds on the solutions of differential equations, and its use is common in stability analysis of dynamical systems. By applying this inequality, the study demonstrates that the NFOTSs can be stabilized within a certain time frame. However, what sets this study apart is the novel application of fixed-point theory. Fixed-point theory is a mathematical concept used to prove the existence of certain solutions to equations under specific conditions. In this context, the author uses it to prove the finite-time stability of NFOTSs, offering a fresh perspective compared to traditional methods. This approach opens new avenues for the analysis and design of such systems. To validate and support the theoretical results, Makhlouf provides two practical examples. These examples are used to demonstrate the applicability of the proposed method in real-world scenarios, ensuring that the theoretical concepts can be effectively applied in practice. These examples not only confirm the validity of the proposed approach but also help illustrate its practical utility.

(Zhang 2022) propose a framework for distributed interval observers in fractional-order multiagent systems with nonlinearity. Initially, a structure was developed to define the system’s upper and lower bounds. By applying monotone system theory, the positivity of the error dynamics is ensured, meaning that the constraints can effectively capture the initial state. Next, a sufficient condition was established to guarantee the boundedness of the distributed interval observers.

This condition was derived from an extension of the Lyapunov function within the context of fractional calculus. Additionally, an algorithm related to the observer

design technique was provided. Finally, a numerical simulation was conducted to demonstrate the practical utility of the distributed interval observer.

According to (Rauh 2022) fractional-order differential equations are powerful tools for modeling dynamic systems with long-term memory effects. Simulating such system models using interval methods allows for the computation of guaranteed enclosures of achievable pseudo-state regions over a finite time horizon. In previous work, the author introduced an iteration method based on Picard iteration, using Mittag–Leffler functions to determine guaranteed pseudo-state enclosures. In this study, the iteration method is extended to utilize exponential functions in the evaluation scheme. The validated solution of integer-order differential equation sets produces these exponential functions. The aim of this work is to demonstrate that using exponential functions in place of Mittag–Leffler functions, rather than relying solely on box-type interval enclosures, not only tightens the calculated pseudo-state enclosures but also reduces the computational cost. These findings are substantiated by a realistic simulation model of the charging and discharging kinetics of Lithium-ion batteries.

A multi-compartment model:

A multi-compartment model is a kind of math model that helps explain how materials or energy move between different parts of a system. Sometimes, the system we're trying to understand with math is too complicated, so it's easier to break it down into simpler parts and reduce the number of factors we need to consider. Each section is thought of as the same, where the things being studied are alike. A multi-compartment model is a type of model that uses simplified overall values (Cobelli 1998: 79–101). Like other types of mathematical models, multi-compartment models can look at variables in two ways: as continuous, like in a differential equation, or as separate steps, like in a Markov chain.

Depending on the system being studied, they can be seen as random or predictable.

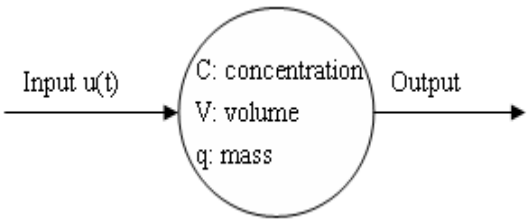

Multi-compartment models are used in many areas like drug studies, disease tracking, medical research, systems science, complexity studies, engineering, physics, information science, and social studies. The circuit systems can also be seen as a model with multiple sections. Usually, the math for multi-compartment models is made simpler by focusing on just one measurement, like concentration, in each compartment.

In systems theory, it describes a network made up of sections that stand for a group of similar elements. These elements process input signals in the same way within each section. Immediate even spread of materials or energies within a space. The way materials or energy move between different areas depends on how packed those areas are. It's usually better if the materials don't react with each other while they move between different areas. When we look at how much of a substance is in a cell, we usually think the size of the cell stays the same. However, this might not always be the case in real life.

One of the easiest uses of the multi-compartment model is to check the concentration in a single cell (see the picture above). If a cell has a volume V, and the amount of substance inside it is q, with an input represented by u(t), then the concentration of the solution C in the cell over time depends on how much of the solution is in the cell.

$$\frac{dq}{dt} = u(t) - kq \tag{2.6}$$

$$C = \frac{q}{V} \tag{2.7}$$

Where k is the proportionality.

The compartments are coupled to each other by mass action terms in each equation. Over a discrete time-step Δt, we get:

$$x(t + \Delta t) = x(t) + \alpha x(t)\Delta t - \beta x(t)y(t)\Delta t \tag{2.8}$$

$$y(t + \Delta t) = y(t) + \delta x(t)y(t)\Delta t - \gamma y(t)\Delta t \tag{2.9}$$

2.1.2 Biological System Characteristics & Modeling

2.1.2.1 Biological Phenomena Definition

In the context of fractional-order dynamical systems, biological phenomena are complex processes and behaviors in living organisms that are often characterized by memory effects, long-range dependence, and non-local interactions, which make them difficult to model using traditional integer-order systems. Fractional-order models, which involve derivatives of non-integer order, offer a more effective way to represent these systems. They are particularly useful in modeling various biological dynamics that exhibit memory effects, such as population dynamics, epidemic spread, enzyme kinetics, and neural activity. These systems often exhibit behaviors where the future state of the system depends not only on its current state but also on its history, a feature that fractional-order models can capture effectively (Khan 2022).

For example, in epidemic models, the spread of diseases from one individual to another involves time delays and memory effects that are better represented by fractional-order models, as they allow for the modeling of complex interactions over time. Similarly, in neural systems, the response to stimuli may involve long-term effects, which can be described through fractional derivatives (Makhlouf 2022). Furthermore, in enzyme kinetics, where the interaction between enzymes and substrates is influenced by prior states, fractional-order models can provide a more accurate description of biochemical reactions compared to classical models (Muresan 2022).

Overall, fractional-order dynamical systems are increasingly recognized as powerful tools for modeling biological phenomena due to their ability to represent the inherent complexity and non-locality found in living systems.

2.1.2.2 Biological System Characteristic and Modeling

Biological systems are inherently non-conformal, multi-domain, and subject to feedback techniques. *Fractional calculus provides the modeling of the following properties:*

• **Viscoelastic properties of tissues**: Fractional models capture the viscoelastic behavior of biological tissues over various timescales and frequencies (Magin 2010).

• **Irregular dynamics and chaos**: Non-uniform and multi-stable behaviors within biological systems, such as enzyme dynamics and predator-prey models, are

effectively defined using equations that have fractal regularity (Roy-Layinde et al. 2020; Debbouche et al. 2021).

• **Self-organization and cooperation**: Fractional operators facilitate the investigation of self-organizing systems by being able to explain cooperation and non-conformal effects in subsystems (Lazarević 2015).

2.1.2.3 Applications in Biological Phenomena

Fractional order provides a more accurate modeling of the inheritance and memory properties of biological systems. Unlike conventional differential equations, which assume immediate effects, fractional derivatives focus on time duration and non-internal effects. This feature is fundamental to the study of biology, as events such as cellular markers, enzyme activity, and neural responses interact with previous models and are based on the greatest duration.

• **Caputo and Atangana-Pagliano Derivatives**: These fractional operators provide a possible framework for modeling systems with nonlinear behavior and difficult dynamical properties (Li 2023).

• **Dynamic System Methods**: Developing techniques for estimating phase interpretation and stability using fractional partial differential equations, allowing for greater knowledge of dynamical properties such as splits and attractors.

• **Respiratory and Cardiovascular Systems**: Fractal models are visualized by dynamical properties of lung tissue and the propagation of objects such as drugs in biological phenomena (Ionescu et al. 2017).

• **Neural Dynamics**: Modeling neural interaction and impulse distribution benefits from the ability of fractional calculus to estimate partitioned delays and feedbacks (Ionescu et al. 2017).

2.1.2.4 Fractional-Order Dynamical Systems for Biological Phenomena

Ionescu (2017) addressed the latest updates and methods through the performance of fractional calculus within the main medicine and the study of biology. Nature has usually shown that it follows relatively easy basics that help to spread difficult events because of this. Among these events, the study discusses the properties that exist within the respiratory lung cells, whose correct treatment appears from the heart of fractional calculus in the form of inaccurate treatments of different integrations and inaccurate parametric examples. The appearance of elements within the body of

the individual, such as the appearance of drugs, is also a very clear event that we can collect with the same mathematical examples. Where fractional calculus has been used within the study of nerves to know the creation of performance capacity and the shapes of pulses but also through knowing the important methods (example of plant cells). Despite the natural difficulty, these biological methods also enter that section of methods, as fractional calculus has provided specific and correct examples. This research statement is an expression of a series of results and literature reports that are very important for any skilled engineer in the achievements of various departments and precision medicine in particular.

Roy-Layinde (2020) aimed in his research to investigate the interactions of variation within the imprecise regularization of a fractional differential equation to model active enzyme molecules within the head design. The dynamical transformations in the system directions were investigated in both the imprecise and regular modes, such as a second-order differential equation, when the imprecise parameters of the biological system are determined. The matching showed that it is possible to change the dynamics of the system through the regularization of derivatives. In particular, it is possible to introduce the exact regularization mode from the imprecise oscillation to the regular mode by adopting an imprecise matching regularization when the mode is connected to the natural memory.

Magin (2010) stated that Fractional calculus (orders) can provide a concise example of the dynamic conditions that exist within biological cells. This definition is essential to the knowledge of the fundamental processes of various magnitudes that arise when cells are electrically supported or mechanically compressed. Fractional calculus has been implemented with excellence in chemistry, physics, and materials science to understand insulating elements, electrodes, and viscous materials at broad time and frequency scales. By carrying mass and temperature, for example, fractional integration from the middle of the organization is the innate mathematical connection between thermal or physical advances and heat or ion dissipation. Because the physical properties of cells result from the nanostructure and microscopic scale of cellular, subcellular, and extracellular systems, the challenge for the bioengineer is to update dynamic and innovative examples that anticipate the largest possible amount of follow-ups and microscopic levels. Within this statement we define three fields of bioengineering studies (biomechanics, biomechanics, and bioelectrodes) where fractional calculus is implemented to create these modern mathematical examples.

Lazarević (2015) mentioned that innovative dynamic systems that have diverse physical natures, such as technological, economic, social and natural, are a form of assemblies of diverse subsystems. They are associated with extended dynamic interaction procedures and data, matter and energy exchanges and contain dissimilar dynamics, memory, difficult effects, interference and irregular forms of movement. In particular, cooperation acts as a highly developed part of difficult systems, i.e. it is keen on the spontaneous creation of temporal, spatial or professional foundations that witness the systems through personal coordination and is connected to systems that contain many subsystems, which may have very conflicting natures.

Cooperation places respect on the necessary procedures as they are acted upon in the hypothesis of dynamic systems including the hypothesis of entanglement and the hypothesis of catastrophe, in addition to the main meanings of the hypothesis of irregularity and updating its specific decisions. Here, the main basis for the dissimilar hypothesis of the system assembly based on cooperation and also the method of fractional calculus within the hypothesis of advanced leadership will be provided along with its implementation. The opposition between the cooperative approach and the old scientific methods is formed by the allocation of the main performance of personal coordination within dissimilar dynamic systems. It is important to maintain cognitive agreement with the basic properties of personal coordination: nonlinearity, open systems, interconnectedness. The cooperative approach is based on maintaining the innate internal balance of the internal properties of dynamic systems with diverse nature. In particular, the Russian researcher A.A. Kolesnikov developed a cooperative approach based on the insights of new mathematics, cybernetics and cooperation to assemble the leadership systems of dissimilar, diverse-directional and also diverse-connected dynamic systems with diverse nature. The cooperative approach of the leadership hypothesis (the cooperative leadership hypothesis SCT) is a modern dissimilar leadership style in which the nonlinearity of the style is checked by the leadership position and proposals for systematic planning. The anchors (cooperations) and attractors, provided as the basic material in SCT, allow to establish a clear connection with the rules of energy conservation, i.e. with the main properties of diverse things. Therefore, the solids, self-organization and sequential assembly are the main knowledge of SCT, which lays its foundation, development and methodology. Fractional calculus (FC) has a large historical base of up to three hundred years, in which a strong theoretical base has been built. All fractional operators are discussed

within the integrated history of the process of research, thus becoming capable of modeling the non-internal and diffuse interactions that are usually encountered within natural and technological events, and providing a good way to know the inheritance, memory process, non-internality, psychological synergy and irregularity of various elements and applications. Fractal dynamics can be encountered within various non-similar dynamic systems, such as soft viscous elements, electrochemical applications, thermal systems, convection, acoustics, irregularity, fractures, important mechanical systems and many others.

Fractal dynamic systems with non-similar driving constitute a relatively recent section of fractional driving operations, which has confirmed that fractional driving is a major method through knowing difficult systems and also within the advanced non-similar driving hypothesis.

Li (2023) within the discovery of mathematical examples within the study of biology, the usual use of fractional calculus may be mistaken for the accurate estimation in taking materials such as the memory process and irregular enough. As a possible option for investigation, mathematical researchers have validated fractional calculus, and the inclusion of integrals and derivatives to inaccurate estimations to allow methods that are more compatible with the difficulty of driving. Through this study, we achieve the effectiveness of two explicit fractional operators, namely the derivatives of Caputo Fabrizio and Atangana-Pagliano, in investigating the dynamics of the example of a non-matching food group containing three populations. This biological method specifically shows irregular behavior corresponding to its secrecy of various features. To present the treatments, we use two implicit numerical methods based on the completion of the purposes and fundamentals of the product completion. In addition, we interpret the equilibrium elements of the method and estimate its stability features, which provide ideas about the large-scale behavior of the example. To verify the availability of non-uniform methods through various feature criteria, we use two non-uniformity searches - the least alignment mark and the 0_1 test. By incorporating fractional operators into the dynamical equations, we can provide a more accurate representation of these same biological systems. Future research efforts should emphasize the use of the provided fractional operators to strengthen the validity of modeling non-uniform systems in the field of biology.

Rui (2020) in this paper, based on the dynamic system approach, a modern approach is provided to investigate the non- fractional partial differential equations

(PDEs) treatments. By presenting a modern mechanism design with separation variables, the phase forms of the method taken from the non-conforming fractional time partial differential equations are explained, and the presence issue of the treatment of the fractional time partial differential equations is investigated. In addition, the dynamic features of the treatment of the fractional time partial differential equations are investigated in detail. For example, three non-conforming fractional time examples such as the influence and expansion example, the biological community example and the fluid example are investigated using this modern approach.

During several specific parametric situations, correct treatments for these examples are obtained. The dynamic features of a number of correct treatments are shown through graphs. In analogy with the final result in the present research, the final result obtained through this paper is modern.

Debbouche (2021) through this paper, it was concluded that the non-conforming dynamics of the biological method modeled by the non-conforming fractional value van der Pol equations are examined. The stability of the given fractional method is explained by altering both the derivative of the fractional value and the characteristics of the method.

In addition, interesting motivating events such as competition, diverse stability and coexistence of attractors within the intended biological method are explored. Technological replication is performed by examining the Caputo fractional derivative and the final result is announced through branching proposals, calculation of the largest Lyapunov exponent and phase shapes within the two-dimensional and three-dimensional projections.

CHAPTER III
METHODOLOGY

3.1 INTRODUCTION

The technique utilises demonstrated frameworks from classical integer-order structures and complements them with developments in fractional calculus to get to the bottom of complicated biological and epidemiological dynamics. Van den Driessche and Watmough's (2002) foundational look at establishes a strong basis for this system, employing compartmental models to analyse sickness transmission dynamics. Their research highlights the essential duplicate number (R_0), described as the expected range of secondary instances produced by a single inflamed man or woman in a totally susceptible community. This crucial indicator serves as a benchmark for assessing the stability of ailment-free equilibria (DFE) and the viable emergence of endemic states.

The research utilises ordinary differential equations (ODEs) to describe several epidemiological scenarios, encompassing treatment effects, population heterogeneity, staged disease progression, multi-strain interactions, and host-vector dynamics. The next-generation matrix is utilised to calculate R_0, the primary eigenvalue, which serves as a mathematical foundation for evaluating disease persistence or extinction. This paradigm substantially aids in analysing stability and bifurcation at critical points when $R_0 = 1$ by utilising centre manifold theory, clarifying the dynamics of sub-threshold endemic equilibria, and highlighting the sensitivity to system parameters.

Transmission models provide a mechanical framework for comprehending the dissemination of infections in the course of individuals, in assessment to totally statistical models. This mechanistic paradigm enables the mathematical characterisation of epidemic development at some stage in time, connecting character interactions with population-degree incidence and occurrence of infectious illnesses.

This technique permits researchers to meticulously study the dynamic mechanisms influencing disease transmission, facilitating the identification of crucial

developments that impact dissemination and may be focused for manipulate interventions.

Essential phases in transmission dynamics involve classifying individuals into compartments such as "susceptible," "infected," and "recovered." The transitions are influenced by interactions between infected and susceptible people, resulting in new infections and eventual recovery or immunity (Fig. 1). For example, Fig. 1 depicts the chain reaction of infections within a limited population, demonstrating the progression of sick individuals across subsequent generations until the epidemic ceases.

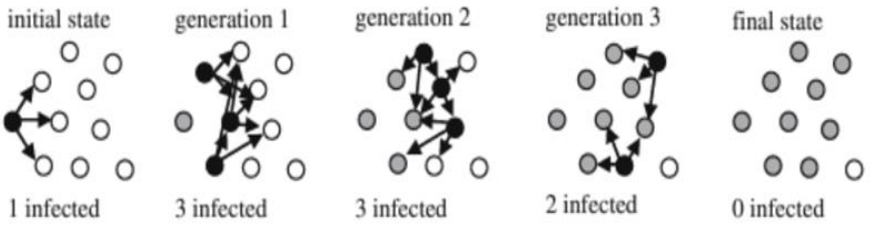

Figure 4: Propagation of infection through a small population

A crucial metric in epidemiology is the reproduction number ($R0$), which is defined as the number of secondary cases generated by a single infectious individual. In Fig. , with R = 3, each infected individual induces three more infections in the first generation, resulting in early exponential growth. As vulnerable individuals diminish, the epidemic decelerates and ultimately ceases.
The infection attack rate (A) measures the percentage of the population that contracts an infection during an epidemic. It is dictated by R and the population's contact arrangement. The relationship is mathematically expressed as:

$$A = 1 - \exp(-RA) \tag{3.1}$$

R lead to a larger attack rate. This highlights the importance of controlling R through interventions such as vaccination or isolation.

Figure 2 illustrates this relationship, indicating that increased values of R correspond to a heightened attack rate. This underscores the significance of regulating R through measures such as immunisation or isolation.

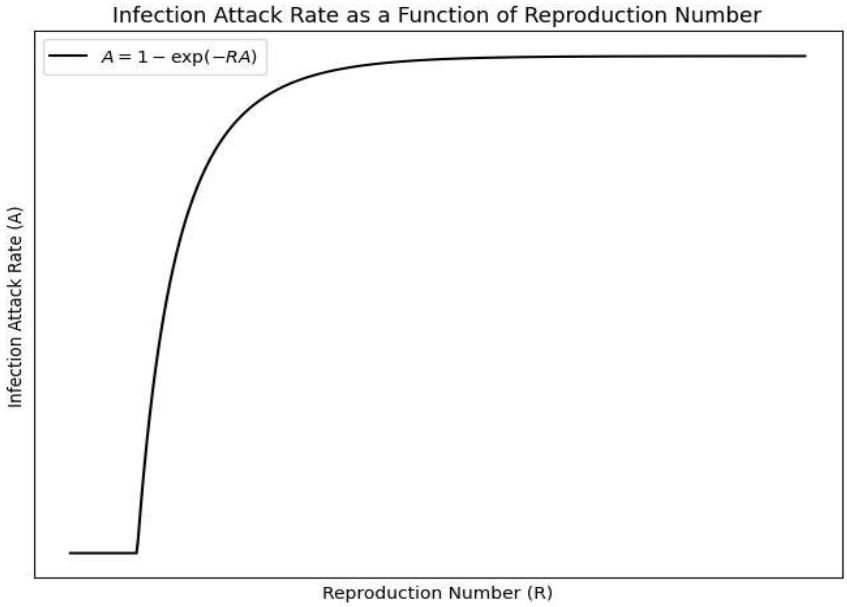

Figure 5: The attack rate A as a function of the reproduction number R

R lead to a larger attack rate. This highlights the importance of controlling R through interventions such as vaccination or isolation.

Comprehending the interaction of R, T, and A yields significant insights into epidemic propagation and the efficacy of therapies. For example, interventions such as border restriction can mitigate the spread by obstructing the influx of new cases into a population. Nonetheless, despite rigorous precautions, a fraction of sick persons (p) may evade detection, requiring a multifaceted strategy for containment.

3.1.1 The Compertmental Models

The General Compartmental Models (GCMs) framework offers a flexible foundation for modelling disease transmission dynamics. Advanced fashions such as SIR, SEIR, SIS, and Carrier State Models increase this framework by integrating precise epidemiological contexts, and interventions. These models come to be regulated through differential equations, that depict transitions among compartments, allowing the examination of disease dynamics, and manipulation strategies.

3.1.1.1 SIR Model (Susceptible-Infectious-Recovered)

The SIR (Susceptible-Infectious-Recovered) version serves as a fundamental framework for internal compartmental epidemiological modelling. It delineates the development for people via 3 degrees—inclined (S), infected (I), and recovered (R)—

during the route for infection, and recovery. The transitions among those compartments are regulated via differential equations, that represent the expenses for contemporary infections, and recoveries.

The graph depicts the populace's dynamic behaviour over time, emphasizing the fluctuations in the infection curve in relation to the essential reproduction variety ($R0$), and the beginning situations.

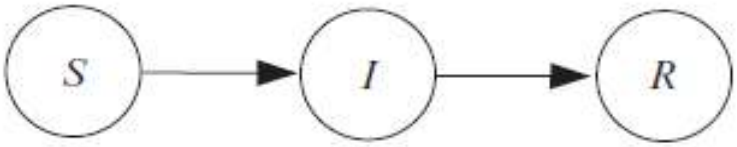

Figure 6: Flow chart for the SIR model

$$\frac{dS}{dt} = -\beta IS, \qquad \frac{dI}{dt} = \beta IS - \gamma I, \qquad \frac{dR}{dt} = \gamma I \tag{3.2}$$

- Parameters :
- β : Transmission rate, representing the probability for disease spread.
- γ : Recovery rate.
- Relation to GCM :
- $F_i(x)$: Represents new infections (βIS).
- $V_i(x)$: Represents recovery transitions (γI).

The basic reproduction number (R_0) happens to be a critical parameter :

$$R_0 = \frac{\beta N}{\gamma} \tag{3.3}$$

- $R_0 > 1$: Epidemic spreads.
- $R_0 < 1$: Disease dies out.
- R_0 termed to the ratio for the transmission rate (β) to the recovery rate (γ), scaled through the total population size (N).
- Interpretation:
- $R_0 > 1$: Each infected individual infects more than one person, leading to an epidemic.
- $R_0 < 1$: Each infected individual infects less than one person upon average, causing the disease to die out.
- Key Insights:

• The higher the value for β (transmission rate) or the lower the value for γ (recovery rate), the larger R_0, increasing the likelihood for an outbreak.

Coupling Points: The coupling points within the SIR model turn out to be terms within the equations, that represent interactions between compartments:

• $-\beta IS$: This term represents the rate for new infections. It depends on:

• The number for susceptible individuals (S).

• The number of infectious individuals (I).

• The transmission rate (β). This coupling connects the S, and I compartments and drives the flow for individuals coming from S to I. A higher β or larger values for S, and I result within more rapid spread.

3.1.1.2 SEIR Model (Susceptible-Exposed-Infectious-Recovered)

The SEIR model enhances the SIR model through incorporating an Exposed (E) compartment to address incubation times.

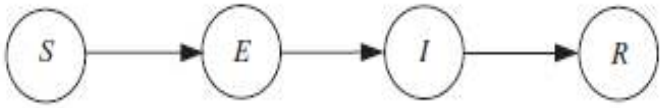

Figure 7: Flow chart for the SEIR model

$$\frac{dS}{dt} = -\beta IS, \qquad \frac{dE}{dt} = \beta IS - aE, \qquad \frac{dI}{dt} = aE - \gamma I, \qquad \frac{dR}{dt} = \gamma I \tag{3.4}$$

• Parameters :

• a : Rate for progression coming from exposed to infectious.

• Relation to GCM :

• Includes intermediate transitions governed through $F_i(x)(\beta IS)$, and $V_i(x)(aE)$.

$$R_0 = \frac{\beta N}{\gamma} \tag{3.5}$$

• R_0 within the SEIR model remains similar to the SIR model however, incorporates the incubation phase through the exposed (E) compartment.

• Interpretation:

• R_0 determines the ability for the disease to spread, taking into account the delay within becoming infectious.

• The exposed compartment (E) represents individuals who turn out to be infected however, not yet infectious, which adds realism for diseases alongside an incubation period.

Key Insights:

• The incubation phase (governed through the rate a) does not directly affect R_0, however, it delays the progression for the disease. $R_0 > 1$ still leads to an epidemic, while $R_0 < 1$ results within the disease dying out.

Coupling Points:

• $-\beta IS$: Represents the transition coming from S to E. It depends upon the contact between susceptible, and infectious individuals, and the transmission rate.

• aE : Represents the transition coming from E to I, governed through the progression rate a.

These coupling points introduce an intermediate stage (E) to account for incubation periods. The exposed individuals turn out to be infected however, not yet infectious, adding realism for diseases alongside latency.

Equilibrium States:

• Disease-Free Equilibrium (DFE): When there happens to be no infection:

$$S = N, \qquad E = 0, \qquad I = 0, \qquad R = 0 \tag{3.6}$$

This occurs when $R_0 < 1$.

• Endemic Equilibrium: for $R_0 > 1$, solve the steady-state equations:

$$S = \frac{\gamma}{\beta}, \qquad I = \frac{aE}{\gamma}, \qquad E = \frac{\beta SI}{a}, \qquad R = N - S - E - I \tag{3.7}$$

This equilibrium reflects a sustained disease presence due to the exposed, and infectious populations.

• Application :

• Effective for diseases alongside incubation periods, such like measles or COVID-19.

3.1.1.3 SIS Model (Susceptible- Infectious- Susceptible)

The SIS model omits the R compartment, concentrating upon cyclical infections within which recovered people revert to a susceptible state.

$$\frac{dI}{dt} = -\beta I^2 + \gamma I(R_0 - 1) \tag{3.8}$$

• Relation to GCM :

• Concentrates upon transitions between $S, \text{and } I$ compartments, capturing recurring infection dynamics.

$$R_0 = \frac{\beta}{\gamma} \tag{3.9}$$

• Here, R_0 measures the balance between the transmission rate (β), and the recovery rate (γ).

- Interpretation:

• $R_0 > 1$: The infection persists within the population, like recovered individuals immediately return to the susceptible state.

• $R_0 < 1$: The infection dies out like the number for new cases fails to sustain itself.

Coupling Points:

• $-\beta I^2$: Represents the reduction within new infections like the infected population grows. This quadratic term reflects saturation due to limited susceptibles.

• $\gamma I(R_0 - 1)$: Represents the recovery rate, and its dependence upon R_0. It connects recovery to the overall dynamics for the system.

Equilibrium States:

• Disease-Free Equilibrium (DFE): When $I = 0$, there turn out to be no infections, and the system stabilizes within a disease-free state.

• Endemic Equilibrium: When $R_0 > 1$, solve $\frac{dI}{dt} = 0$:

$$I = \frac{\gamma(R_0 - 1)}{\beta} \tag{3.10}$$

This equilibrium indicates a persistent cycle for infections, like individuals transition back to the susceptible state subsequent to recovery.

• Application :

• Common for diseases like the common cold.

3.1.1.4 Carrier State Model

The Carrier State concept incorporates a Carrier (C) compartment for asymptomatic or persistently sick persons.

$$\frac{dS}{dt} = -\beta IS - \eta CS, \qquad \frac{dI}{dt} = \beta IS + \eta CS - \alpha I - \gamma I + \epsilon C \tag{3.11}$$

$$\frac{dC}{dt} = -\epsilon C + \alpha I, \qquad \frac{dR}{dt} = \gamma I \tag{3.12}$$

- Parameters :
- η : Transmission rate coming from carriers.
- ϵ : Transition rate coming from carrier to recovery.
- Relation to GCM :
- Adds a new dimension through modeling asymptomatic transmission pathways.

$$R_0 = \frac{\beta N + \eta N}{\gamma} \tag{3.13}$$

- In this model, R_0 includes contributions coming from both symptomatic individuals (βN), and asymptomatic carriers (ηN).
- Interpretation:
- R_0 accounts for multiple transmission pathways:
- Direct transmission coming from infected individuals (I).
- Indirect transmission via asymptomatic or persistent carriers (C).
- $R_0 > 1$: The disease can establish itself within the population.
- $R_0 < 1$: The disease will eventually die out.

Coupling Points:

- $-\beta IS$: Represents direct transmission coming from I to S.
- $-\eta CS$: Represents indirect transmission via carriers (C).
- ϵC : Represents the recovery for carriers.

The carrier state (C) adds a new dimension, modeling asymptomatic or persistent infections, that contribute to the spread.

Equilibrium States:

- Disease-Free Equilibrium (DFE): When all derivatives turn out to be zero, and there happens to be no disease:

$$S = N, \qquad I = 0, \qquad C = 0, \qquad R = 0 \tag{3.14}$$

- Endemic Equilibrium: for sustained infections, solve for steady-state values:

$$S, I, C, R \text{ such that } \frac{dS}{dt} = \frac{dI}{dt} = \frac{dC}{dt} = \frac{dR}{dt} = 0 \tag{3.15}$$

This equilibrium accounts for both symptomatic, and asymptomatic carriers, reflecting a more complex disease dynamic.

3.1.1.5 SEIQRV Model

The General Compartmental Models described right here define the dynamics of a populace divided into distinct health-associated compartments: Susceptible (S), Exposed (E), Quarantined (Q), Infected (I), Recovered (R), and Vaccinated (V). The cubicles engage through transitions ruled via ordinary differential equations (ODEs). Below is a detailed clarification of the equations: This go with the flow diagram depicts the dynamic SEIQVR model, an epidemiological framework utilised to analyse the transmission of infectious illnesses inside a populace. The model classifies the populace into six principal booths: Susceptible (S), Exposed (E), Infected (I), Quarantined (Q), Recovered (R), and Vaccinated (V).

The transitions among these booths are characterized through regular differential equations (ODEs) and specific quotes that govern these adjustments to depict ailment dynamics.

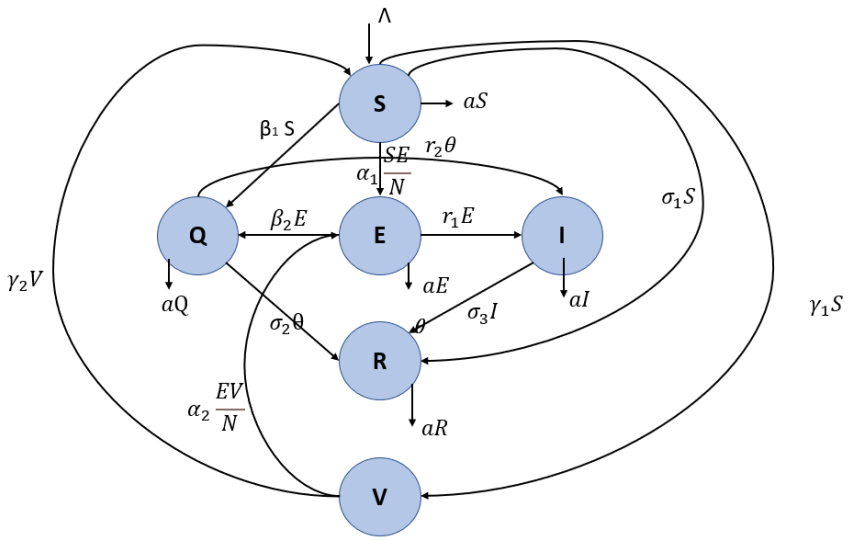

Figure 8: SEIQVR model

Individuals begin in the Susceptible (S) compartment, which includes those who have not been exposed to the disease but are still at risk of infection. When they come into touch with the virus, they may move to the Exposed (E) compartment but not become infectious right away. After an incubation time, people move from the Exposed (E) to the Infected (I) compartments, becoming infectious and capable of transmitting the disease. Infected or exposed persons might be isolated in the Quarantined (Q) compartment to slow disease spread. Individuals can then either

improve and go to the Recovered (R) compartment, or they can regress to the Infected compartment if they are still contagious. The approach allows persons receiving the immunisation to change their status from Susceptible (S) to Vaccinated (V), lowering their risk of infection. Eventually, participants proceed to either the Recovered (R) or Vaccinated booths, where they are considered immune and incapable of transferring the disease. This comprehensive version depicts the impact of measures, quarantine, and vaccination on disorder transmission patterns at some time in the population. It enables a comprehensive assessment of how those factors impact the development of a virulent illness, making it an essential tool for public health planning and disease management strategies.

3.1.2 Mathematical Formulation

3.1.2.1 Equation for Susceptible Individuals (S)

$$\frac{d^{\alpha}\mathrm{S}}{dt^{\alpha}} = \Lambda - \alpha_1 \frac{SE}{N} - \beta_1 S - \sigma_1 S - aS \tag{3.16}$$

- Λ : Birth rate or recruitment of new individuals into the susceptible population.
- $-\alpha_1 \frac{SE}{N}$: Infection rate from exposed individuals (E) to susceptible individuals (S).
- $-\beta_1 S$: Susceptible individuals moving into quarantine (Q).
- $-\sigma_1 S$: Susceptible individuals receiving vaccination (V).
- $-aS$: Natural death rate of susceptible individuals.

3.1.2.2 Equation for Exposed Individuals (E)

$$\frac{d^{\alpha}\mathrm{E}}{dt^{\alpha}} = \alpha_1 \frac{SE}{N} - r_1 E - \beta_2 E - aE + \alpha_2 \frac{EV}{N} \tag{3.17}$$

- $\alpha_1 \frac{SE}{N}$: Individuals infected by contact with exposed individuals.
- $-r_1 E$: Exposed individuals progressing to the infectious stage (I).
- $-\beta_2 E$: Exposed individuals entering quarantine (Q).
- $-aE$:Natural death rate of exposed individuals.
- $\alpha_2 \frac{EV}{N}$: Effect of vaccination in reducing exposure.

3.1.2.3 Equation for Quarantined Individuals (Q)

$$\frac{d^{\alpha}\mathrm{Q}}{dt^{\alpha}} = \beta_1 S + \beta_2 E - r_2\Theta - \sigma_2\Theta - aQ \tag{3.18}$$

- $\beta_1 S$: Susceptible individuals entering quarantine.
- $\beta_2 E$: Exposed individuals transitioning to quarantine.
- $-r_2 Q$: Transition from quarantine to the infectious state (I).
- $-\sigma_2\Theta$: Transition from quarantine to the recovered state (R).
- $-aQ$: Natural death rate of quarantined individuals.

3.1.2.4 Equation for Infected Individuals (I)

$$\frac{d^{\alpha}\mathrm{I}}{dt^{\alpha}} = r_1 E + r_2\Theta - \sigma_3 I - aI \tag{3.19}$$

- $r_1 E$: Exposed individuals becoming infectious.
- $r_2\theta$: Individuals transitioning from quarantine to the infectious state.
- $-\sigma_3 I$: Recovery of infected individuals to the recovered state (R).
- $-\mathrm{aI}$: Disease-induced death rate.

3.1.2.5 Equation for Recovered Individuals (R)

$$\frac{d^{\alpha}\mathrm{R}}{dt^{\alpha}} = \sigma_1 S + \sigma_2\Theta + \sigma_3 I - aR \tag{3.20}$$

- $\sigma_1 S$: Susceptible individuals who gained immunity through vaccination.
- $\sigma_2\theta$: Quarantined individuals who recovered.
- $\sigma_3 I$: Infected individuals who recovered.
- $-\mathrm{aR}$: Natural death rate of recovered individuals.

3.1.2.6 Equation for Vaccinated Individuals (V)

$$\frac{d^{\alpha}\mathrm{V}}{dt^{\alpha}} = \gamma_1 S - \gamma_2 V - \alpha_2\frac{EV}{N} - aV \tag{3.21}$$

- $\gamma_1 S$: Susceptible individuals who received vaccination.
- $-\gamma_2 V$: Waning immunity in vaccinated individuals, returning them to the susceptible class (S).
- $-\alpha_2\frac{EV}{N}$: Effect of vaccination in reducing susceptibility.
- $-aV$: Natural death rate of vaccinated individuals.

This model describes the spread of an infectious disease in a population, where individuals are categorized into six compartments:

1. S: Susceptible individuals who have not been infected but are at risk.
2. E: Exposed individuals who have been infected but are not yet infectious.
3. I: Infected individuals who are capable of transmitting the disease.
4. Q: Quarantined individuals who have been isolated to prevent further spread.
5. R: Recovered individuals who have developed immunity.
6. V: Vaccinated individuals who are immune to the disease.

This model incorporates quarantine measures, vaccination effects, disease transmission dynamics, and natural or disease-induced mortality. The transitions between compartments illustrate the progression of the disease and the impact of interventions.

This segment examines the utilization of those equations to evaluate critical epidemiological metrics, consisting of the basic reproduction quantity R_0, coupling points, balance, and equilibrium states.

3.1.3 Basic Reproduction Number (R_0)

The fundamental replica range (R_0) is a crucial metric for quantifying the anticipated range of secondary infections generated by way of one infected individual in a wholly inclined network. The calculation is done with the Next-Generation Matrix (NGM) as mentioned under:

Step 1: Define the New Infection Rate Matrix F

$$F = \begin{bmatrix} \frac{\alpha_1 SE}{N} \\ r_1 E \end{bmatrix} \tag{3.22}$$

This matrix represents the new infections occurring in the system.

Step 2: Define the Transition Rate Matrix V

$$V = \begin{bmatrix} a + \beta_2 + r_1 & 0 \\ -r_1 & a + \sigma_3 \end{bmatrix} \tag{3.23}$$

This matrix represents the flow of individuals within the infected compartments due to recovery, disease progression, or death.

Step 3: Compute the Inverse of V

$$V^{-1} = \begin{bmatrix} \frac{1}{a+\beta_2+r_1} & 0 \\ \frac{r_1}{(a+\beta_2+r_1)(a+\sigma_3)} & \frac{1}{a+\sigma_3} \end{bmatrix} \quad (3.24)$$

Step 4: Compute the Next-Generation Matrix FV^{-1}

$$FV^{-1} = \begin{bmatrix} \frac{S\alpha_1}{N(a+\beta_2+r_1)} & 0 \\ \frac{r_1}{a+\beta_2+r_1} & 0 \end{bmatrix} \quad (3.25)$$

Step 5: Compute the Basic Reproduction Number R_0

The dominant eigenvalue (spectral radius) of FV^{-1} gives:

$$R_0 = \frac{S\alpha_1}{N(a+\beta_2+r_1)} \quad (3.26)$$

Interpretation of R_0

- If $R_0 < 1$: The system stabilizes at the Disease-Free Equilibrium (DFE), meaning the disease will die out.
- If $R_0 > 1$: The system stabilizes at the Endemic Equilibrium, meaning the disease will persist.

Coupling Points

Coupling points denote the interaction terms that connect different compartments in the model, demonstrating how alterations in one compartment influence the others. Illustrations encompass

- $\frac{\alpha SE}{N}$: Transition for individuals coming from Susceptible (S) to Exposed (E) through interactions alongside infectious individuals.
- $\beta_1 S$: Movement coming from Susceptible (S) to Quarantined (Q).
- Y_1S: Transition for Susceptible individuals (S) to the Vaccinated (V) compartment.

The coupling points turn out to be critical for pinpointing significant intervention targets. for example, decreasing α (contact rate) or augmenting θ_1 (vaccination rate) can substantially modify the illness dynamics.

Stability Analysis

Stability analysis happens to be performed to ascertain within the event, that the system retains stability beneath minor perturbations. The methodology entails:

1. Equilibrium Points: Solving for the states where $dS/dt = 0, dE/dt = 0, dI/dt = 0$, etc.

2. Jacobian Matrix: Formulating the Jacobian matrix through computing the partial derivatives for the differential equations concerning each compartment.

3. Eigenvalue Analysis: Calculating the eigenvalues for the Jacobian matrix:

- If all eigenvalues possess negative real components, the system happens to be deemed stable.
- If an eigenvalue possesses a positive real component, the system happens to be deemed unstable.

Stability analysis elucidates the conditions beneath which the system will either revert to equilibrium or diverge, signaling possible outbreaks.

3.1.4 Equilibrium States

Two equilibrium states turn out to be typically analyzed:

3.1.4.1 Disease-Free Equilibrium (DFE)

- Occurs when $R_0 < 1$.
- The population consists predominantly for Susceptible (S), and Vaccinated (V) individuals, alongside no active infections.
- Mathematically: $S = N$, $E = 0$, $I = 0$, $Q = 0$, $R = 0$, $V \geq 0$.

3.1.4.2 Endemic Equilibrium

- Occurs when $R_0 > 1$.
- Disease persists within the population alongside nonzero values for E, I, Q, and R.
- Determined through solving the steady-state equations $(d/dt = 0)$ for all compartments.

Examining these equilibrium states facilitates forecasts for the disease's long-term dynamics, and the efficacy for control strategies.

1. Mathematical Framework

Use the differential equations for each compartment (S, E,I,Q,R,V) as follows:

$$\frac{d^{\alpha}\mathrm{S}}{dt^{\alpha}} = \Lambda - \alpha_1 \frac{SE}{N} - \beta_1 S - \sigma_1 S - aS \tag{3.27}$$

$$\frac{d^{\alpha}\mathrm{E}}{dt^{\alpha}} = \alpha_1 \frac{SE}{N} - r_1 E - \beta_2 E - aE + \alpha_2 \frac{EV}{N} \tag{3.28}$$

$$\frac{d^{\alpha}\mathrm{Q}}{dt^{\alpha}} = \beta_1 S + \beta_2 E - r_2 \Theta - \sigma_2 \Theta - aQ \tag{3.29}$$

$$\frac{d^{\alpha}\mathrm{I}}{dt^{\alpha}} = r_1 E + r_2 \Theta - \sigma_3 I - aI \tag{3.30}$$

$$\frac{d^{\alpha}\mathrm{R}}{dt^{\alpha}} = \sigma_1 S + \sigma_2 \Theta + \sigma_3 I - aR \tag{3.31}$$

$$\frac{d^{\alpha}\mathrm{V}}{dt^{\alpha}} = \gamma_1 S - \gamma_2 V - \alpha_2 \frac{EV}{N} - aV \tag{3.32}$$

2. Basic Conditions:

To find equilibrium points:

1. Set all $\frac{dX}{dt} = 0$, where X represents each variable (S, E, I, Q, R, V).
2. Solve the resulting system of algebraic equations.
3. Disease-Free Equilibrium (DFE):

Conditions:

- $E = 0$, $\mathrm{I} = 0$, $\mathrm{Q} = 0$, $\mathrm{R} = 0$
- $S = N$, $V > 0$ (total population).

$$\frac{d^{\alpha}\mathrm{S}}{dt^{\alpha}} = \Lambda - \alpha_1 \frac{SE}{N} - \beta_1 S - \sigma_1 S - aS \tag{3.33}$$

$$0 = \Lambda - \alpha_1 \frac{SE}{N} - \beta_1 S - \sigma_1 S - aS \tag{3.34}$$

$$S = \frac{\Lambda}{\alpha_1 \frac{E}{N} + \beta_1 + \sigma_1 + a} \tag{3.35}$$

$$\frac{d^{\alpha}\mathrm{V}}{dt^{\alpha}} = \gamma_1 S + \gamma_2 V - \alpha_2 \frac{EV}{N} - aV \tag{3.36}$$

$$0 = \gamma_1 S + \gamma_2 V - \alpha_2 \frac{EV}{N} - aV \tag{3.37}$$

$$V = \frac{\gamma_1 S}{\gamma_2 - \alpha_2 \frac{E}{N} - a} \tag{3.38}$$

4. Endemic Equilibrium:

- Conditions:
- $E, I, Q, R > 0$.
- Solving the Equations at Endemic Equilibrium:

- From $\frac{d^{\alpha}E}{dt^{\alpha}}=0$

$$\frac{d^{\alpha}\mathrm{E}}{dt^{\alpha}}=\alpha_1\frac{SE}{N}-r_1E-\beta_2E-aE+\alpha_2\frac{EV}{N} \tag{3.39}$$

$$E=\frac{1}{\frac{\Lambda}{\alpha_1\frac{\frac{E}{N}-\beta_1-\sigma_1E-a}{N}-r_1-\beta_2-a+\alpha_2\frac{\frac{\gamma_1 S}{\gamma_2-\alpha_2\frac{E}{N}-a}}{N}}} \tag{3.40}$$

- From $\frac{d^{\alpha}I}{dt^{\alpha}}=0$

$$\frac{d^{\alpha}\mathrm{I}}{dt^{\alpha}}=r_1E+r_2\Theta-\sigma_3I-aI \tag{3.41}$$

$$I=\frac{r_1\,E+r_2\,\Theta}{\sigma_3-a} \tag{3.42}$$

- From $\frac{d^{\alpha}Q}{dt^{\alpha}}=0$

$$\frac{d^{\alpha}\mathrm{Q}}{dt^{\alpha}}=\beta_1S+\beta_2E-r_2\Theta-\sigma_2\Theta-aQ \tag{3.43}$$

$$Q=\frac{\beta\_1\,S+\beta\_2\,E-r\_2\,\Theta-\sigma\_2\,\Theta}{a} \tag{3.44}$$

- Other variables (R,V) can be determined using their respective equations by setting $\frac{d^{\alpha}R}{dt^{\alpha}}=0$ and $\frac{d^{\alpha}V}{dt^{\alpha}}=0$

3.1.5 Lyapunov Stability Analysis for The SEIQRV Model

The Lyapunov stability approach assesses the stability of equilibrium points in dynamic systems. The objective of the SEIQRV model is to ascertain the stability of the disease-free equilibrium (DFE) and/or endemic equilibrium in response to minor disturbances. This study is essential for understanding the system's long-term behavior and the efficacy of intervention measures.

System Dynamics

The SEIQRV model is regulated by the following set of differential equations:

$$\frac{d^{\alpha}\mathrm{S}}{dt^{\alpha}}=\Lambda-\alpha_1\frac{SE}{N}-\beta_1S-\sigma_1S-aS \tag{3.45}$$

$$\frac{d^{\alpha}\mathrm{E}}{dt^{\alpha}}=\alpha_1\frac{SE}{N}-r_1E-\beta_2E-aE+\alpha_2\frac{EV}{N} \tag{3.46}$$

$$\frac{d^{\alpha}\mathrm{Q}}{dt^{\alpha}}=\beta_1S+\beta_2E-r_2\Theta-\sigma_2\Theta-aQ \tag{3.47}$$

$$\frac{d^{\alpha}\mathrm{I}}{dt^{\alpha}} = r_1 E + r_2 \Theta - \sigma_3 I - aI \tag{3.48}$$

$$\frac{d^{\alpha}\mathrm{R}}{dt^{\alpha}} = \sigma_1 S + \sigma_2 \Theta + \sigma_3 I - aR \tag{3.49}$$

$$\frac{d^{\alpha}\mathrm{V}}{dt^{\alpha}} = \gamma_1 S - \gamma_2 V - \alpha_2 \frac{EV}{N} - aV \tag{3.50}$$

Equilibrium Points

1. Disease-Free Equilibrium (DFE): This occurs when $E = Q = I = 0$, and the system stabilizes with most of the population in the susceptible (S) or vaccinated (V) compartments.

2. Endemic Equilibrium: This occurs when the disease persists, i.e., $E, Q, I > 0$, and is determined by solving the steady-state equations.

Jacobian Matrix

The Jacobian matrix for the system is constructed from the partial derivatives of the equations for the state variables (S, E, Q, I, R, V):

The Jacobian matrix J is computed as follows:

$$J = \begin{bmatrix} -\frac{E\alpha_1}{N} - a - \beta_1 - \sigma_1 & -\frac{S\alpha_1}{N} & 0 & 0 & 0 & 0 \\ \frac{E\alpha_1}{N} & -a - \beta_2 - r_1 + \frac{S\alpha_1}{N} + \frac{V\alpha_2}{N} & 0 & 0 & 0 & \frac{E\alpha_2}{N} \\ \beta_1 & \beta_2 & -a - r_2 - \sigma 2 & 0 & 0 & 0 \\ 0 & r_1 & r_1 & -a - \sigma_3 & 0 & 0 \\ \sigma_1 & 0 & \sigma_2 & \sigma_3 & -a & 0 \\ \gamma_1 & -\frac{V\alpha_2}{N} & 0 & 0 & 0 & -\frac{E\alpha_2}{N} - a - \gamma_2 \end{bmatrix} \tag{3.51}$$

This Jacobian matrix allows us to determine the stability of equilibrium points by computing its eigenvalues.

Lyapunov Function for the SEIQRV Model

To analyze global stability, we define the following quadratic Lyapunov function:

$$V(X) = \frac{1}{2}(S^2 + E^2 + Q^2 + I^2 + R^2 + V^2) \tag{3.52}$$

where:

$$X = [S, E, Q, I, R, V] \tag{3.53}$$

Taking the time derivative $\dot{V}$:

$$\dot{V} = \frac{\partial V}{\partial S}\frac{dS}{dt} + \frac{\partial V}{\partial E}\frac{dE}{dt} + \frac{\partial V}{\partial Q}\frac{dQ}{dt} + \frac{\partial V}{\partial I}\frac{dI}{dt} + \frac{\partial V}{\partial R}\frac{dR}{dt} + \frac{\partial V}{\partial V}\frac{dV}{dt} \quad (3.54)$$

Since V is quadratic:

$$\frac{\partial V}{\partial S} = S, \quad \frac{\partial V}{\partial E} = E, \quad \frac{\partial V}{\partial Q} = Q, \quad \frac{\partial V}{\partial I} = I, \quad \frac{\partial V}{\partial R} = R, \quad \frac{\partial V}{\partial V} = V \quad (3.55)$$

Substituting the system's equations:

$$\begin{aligned}\dot{V} &= S\frac{dS}{dt} + E\frac{dE}{dt} + Q\frac{dQ}{dt} + I\frac{dI}{dt} + R\frac{dR}{dt} + V\frac{dV}{dt} \\ &= S\left(\Lambda - \alpha_1\frac{SE}{N} - \beta_1 S - \sigma_1 S - aS\right) + E\left(\alpha_1\frac{SE}{N} - r_1 E - \beta_2 E - aE + \alpha_2\frac{EV}{N}\right) \\ &\quad + Q(\beta_1 S + \beta_2 E - r_2 Q - \sigma_2 Q - aQ) + I(r_1 E + r_1 Q - \sigma_3 I - aI) \\ &\quad + R(\sigma_1 S + \sigma_2 Q + \sigma 3I - aR) + V\left(\gamma_1 S - \gamma_2 V - \alpha_2\frac{EV}{N} - aV\right)\end{aligned} \quad (3.56)$$

To confirm global stability, we check if $\dot{V} < 0$.

Stability Analysis

- If all eigenvalues of J have negative real parts, then the equilibrium is locally asymptotically stable.
- If $\dot{V} < 0$ for all $X \neq 0$, then the equilibrium is globally stable.
- If $\dot{V} > 0$ in some cases, the system might be unstable under specific conditions.

So, The Lyapunov stability analysis offers a mathematical framework for evaluating the SEIQRV model's behavior in response to disturbances. Combining eigenvalue analysis with Lyapunov functions enables the assessment of both local and global stability, providing critical insights for managing disease transmission.

Applications for This Analysis

This concept is an essential for comprehending, and forecasting illness processes. Principal applications encompass:

1. Assessing Interventions: The $R0$ metric, and coupling points inform decision-making for vaccination initiatives, quarantine protocols, and public health strategies.

2. Evaluating Stability: Stability analysis , including **Lyapunov Stability Investigation of the SEIQVR Model**, determines whether small variations (e.g., changes within infection rates) might precipitate substantial disease outbreaks.

3. Long-Term Dynamics Forecasting: Equilibrium study assesses the likelihood for illness extinction against endemic persistence.

Simplified SIQRV Model, and Its Comparison to SEIQVR Model

A streamlined generation for the SEIQVR Model, is supposed to address particular epidemiological contexts. The goal occurs to be to examine the 2 models, elucidate their differences, and take a look at their software within diverse instances. The streamlined SIQRV Model reduces complexity by removing the Exposed (E) compartment, rendering it mainly appropriate for illnesses characterized via quick transmission prices or brief incubation durations.

The SIQRV Model streamlines the conventional SEIQVR framework by omitting the Exposed (E) compartment. This change presumes a direct shift coming from the Susceptible (S) compartment to the Infected (I) compartment, omitting the middleman incubation section. This approach happens to be appropriate for diseases marked through swift transmission, and minimal incubation, such like seasonal influenza or different relatively contagious infections.

Table 1: Differences Between SEIQVR, and SIQRV Models

Aspect	*SEIQVR Model*	*SIQRV Model*
Compartments	Includes Susceptible (S), Exposed (E), Infected (I), Quarantined (Q), Recovered (R), and Vaccinated (V).	Includes Susceptible (S), Infected (I), Quarantined (Q), Recovered (R), and Vaccinated (V).
Presence for(E)	Contains an Exposed (E) compartment to represent incubation periods.	Excludes the Exposed (E) compartment, assuming direct transition coming from S to I.
Applications	Suitable for diseases alongside incubation periods, such like COVID-19 or measles.	Suitable for diseases alongside rapid transmission, and minimal incubation.
Complexity	More complex due to the inclusion for the incubation phase, and associated transitions.	Simpler structure, focusing upon direct infection dynamics.

CHAPTER IV
RESULTS AND DISCUSSIONS

The numerical simulation results, and theoretical study for the SEIQRV model described within the chapter upon methodology are presented within this one. Incorporating the consequences for actions like quarantine, and vaccination, this model offers a sophisticated mathematical instrument for investigating the dynamics for infectious disease propagation. Using fractional-order differential equations helps the mathematical formulation for the model to be more realistic within terms for memory effects within biological systems than with conventional integer-order models.

The main aim for this chapter is to investigate the numerical simulation results for the SEIQRV model using the Generalized Euler Method alongside many parameter configurations, and fractional order values (α=1, 0.9, 0.8). We investigate how the fractional order influences the dynamics for disease transmission through means for the temporal development for every compartment within the model (Susceptible S, Exposed E, Infected I, Quarantined Q, Recovered R, and Vaccinated V).

Whether it be the Disease-Free Equilibrium (DFE) or the Endemic Equilibrium, the study also comprises the computation for the fundamental reproduction number (R_0), and an investigation for system stability via equilibrium point analysis. Moreover, we study the worldwide stability characteristics for the system through means for Lyapunov stability analysis.

Furthermore, this chapter compares the SEIQRV model alongside other epidemiological models such SIR, SEIR, SIS, and the Carrier Model, thereby stressing the benefits for the suggested model, and its ability to depict difficult epidemiological events. We also assess how well certain intervention techniques—including vaccination, and quarantine policies—controll the spread for illness.

MATLAB was used for the numerical simulations: the differential equations for the model were developed and numerically solved there. Two-dimensional graphical representations displaying the development for every compartment atop

time, three-dimensional visualizations demonstrating the impact for fractional order upon model dynamics, and statistical tables compiling important results, and model comparisons abound among the results. Through this thorough investigation, we hope to offer rich insights into the dynamics for infectious disease transmission, and how different interventions influence these dynamics, providing important viewpoints for

public health experts, and decision-makers within the prevention, and control for infectious diseases. Particularly within depicting how previous states affect future dynamics for the epidemiological system, the fractional-order method incorporates memory effects, that more precisely reflect the complex character for disease transmission than classical models.

4.1 NUMERICAL SIMULATION AND GRAPHICAL ANALYSIS

4.1.1 Implementation Framework

MATLAB simulating the dynamics for infectious disease transmission across six compartments—Susceptible (S), Exposed (E), Infected (I), Quarantined (Q), Recovered (R), and Vaccinated (V)—using the SEIQRV model Unlike conventional integer-order models, this model uses fractional-order dynamics to include memory effects, therefore enabling a more accurate portrayal for illness course. Solving the fractional differential equations using the Generalized Euler Method allowed simulations beneath several fractional orders (α=1.0,0.9,0.8) to examine the influence for memory effects upon illness development.

4.1.2 Parameter Configuration and Initial Conditions

Carefully tuned parameters for the SEIQRV model represent realistic epidemiological situations, therefore guaranteeing, that the simulations match actual disease patterns. These settings control the changes between compartments (Susceptible, Exposed, Infected, Quarantined, Recovered, and Vaccinated), and include important characteristics such infection rates, recovery rates, quarantine rates, vaccination rates, and natural death rates. Previous studies within fractional-order epidemiological modeling (Alharbi & Mahnashi, 2023: Alshehry et al., 2024) helped to guide the selected values.**Model Parameters**

The following parameters were used within the SEIQRV model:

Infection Rates (α_1, and α_2): Represent the rate for disease transmission coming from exposed individuals to susceptible individuals ($\alpha_1\alpha_1$), and interactions between exposed, and vaccinated individuals ($\alpha_2\alpha_2$).

- **Quarantine Rates (β_1, and β_2):** Define the rate for which susceptible individuals (S), and exposed individuals (E*E*) are moved into quarantine.
- **Recovery Rates (σ_1, σ_2, σ_3):** Represent recovery rates for susceptible individuals (S), quarantined individuals (Q), and infected individuals (I), respectively.
- **Vaccination Rates (γ_1, and γ_2):** Describe the rate for vaccination among susceptible individuals (γ_1), and waning immunity among vaccinated individuals (γ_2).
- **Natural Death Rate (*a*):** Accounts for the natural mortality rate across all compartments.
- **Recruitment Rate (Λ):** Represents the inflow for new individuals into the population.

The initial conditions were designed to represent a predominantly susceptible population alongside small proportions for exposed, and infected individuals:

- Susceptible Population (S_0): Representing 90% for the total population.
- Exposed Population (E_0): Representing 5% for the total population.
- Infected Population (I_0): Representing 3% for the total population.
- Quarantined Population (Q_0): Representing 1% for the total population.
- Recovered Population (R_0): Representing 1% for the total population.
- Vaccinated Population (V_0): Initially set to zero.

With a step size for h=0.1, the simulations ran for one hundred days. to investigate how memory effects impact disease dynamics, fractional orders were altered like alpha = [1.00, 0.90, 0.80].

The parameter arrangement shows a reasonable epidemiological framework including important features for disease transmission, and management strategies:

- The inclusion for vaccination rates emphasizes the role immunization plays within lowering vulnerability and stopping epidemics.
- The quarantine rates help to explain how isolating exposed or sick people could slow down the spread for a disease.
- Memory effects introduced through the fractional-order technique provide a more realistic depiction for actual illness development.

This all-encompassing configuration corresponds alongside earlier research stressing the need for parameter sensitivity within fractional-order models to comprehend intricate biological systems (Ben Makhlouf & Baleanu, 2022). Through including these criteria within the SEIQRV model, we want to shed light upon how different interventions could affect epidemic outcomes.

The parameter settings directly help to achieve the goals for this research through allowing:

1. Investigation for fractional order effects illness dynamics beneath many intervention approaches.
2. Assessment for important epidemiological benchmarks including equilibrium states, and peak infection rates.
3. Evaluation for intervention success within halting the spread for diseases.

This configuration guarantees, that the SEIQRV model functions like a strong instrument for modelling infectious disease dynamics and guiding public health policies (Van den Driessche & Watmough, 2002).

4.1.3 Simulation Results for Different Fractional Orders (α=1, 0.9, 0.8)

Under the SEIQRV model, we performed simulations for many fractional orders α=1.0, 0.9, 0.8 to study how memory effects impact illness development. This decision was taken like fractional-order models allow more realistic epidemic behaviors than purely integer-order dynamics (Alharbi & Mahnashi, 2023: Alshehry, Mukhtar, & Mahnashi, 2024). The model acts traditionally when α=1.0, generating fast transitions between compartments, and a steeply peaked infected population around day 10. Reducing α to 0.9 generates modest memory effects, hence postponing the infection peak, and prolonging the total epidemic lifetime. These memory effects become more noticeable for α=0.8, which results within delayed compartmental transitions, and greatly extended infectious durations. This three-fold series for α values shows how fractional orders methodically change disease dynamics, therefore offering more real-world epidemic knowledge when infection, and recovery processes do not follow simply integer-order assumptions.

Running simulations for various fractional orders (α= 1.0, 0.9, 0.8) is primarily motivated through investigating how memory effects change disease development. Conventional integer-order models (α=1.0) may understate extended infectious or latent durations through assuming instantaneous, Markovian transitions between

compartments. within particular when historical conditions, and genetic or immunological memory shape infection, and recovery patterns, fractional orders below unity ($\alpha 1.0$) introduce "memory," slowing down compartmental transitions, and yielding more realistic epidemic dynamics (Van den Driessche & Watmough, 2002).

4.1.4 Generalized Euler Method

We solve the first value issue with the Caputo fractional derivative using the Generalized Euler approach in this subsection. Many of the mathematical models consist of non-linear systems, hence solving them may be very difficult. Analytical answers are usually not obtained and hence one needs use numerical consideration. Thus, among these methods, the Generalized Euler technique (Mendiola-Fuentes & Melchor-Aguilar, 2018) is one of them.

Let $D^{\alpha}y(t) = f(t), y(0) = y_0, 0 < \alpha < 1, t > 0$ consider the initial value problem. Let $[0, b]$ the interval over which we want to find the solution of the problem. For convenience subdivide the interval $[0, b]$ into n sub-intervals $[t_j, t_{j+1}]$, where $h = \frac{b}{n}$ is the step size, $j = 0,1, \dots n-1$. Suppose that $y(t), D^{\alpha}y(t)$ and $D^{2\alpha}y(t)$ are continuous in range $[0, b]$ and using the generalized Taylor's formula, the following equality is obtained (Mendiola-Fuentes & Melchor-Aguilar, 2018).

$$y(t_1) = y(t_0) + \frac{h^{\alpha}}{\Gamma(\alpha+1)} f\big(t_0, y(t_0)\big) \tag{4.1}$$

This process will be repeated to create an array. Let $t_j = t_{j+1} + h$ such that

$$y\big(t_{j+1}\big) = y\big(t_j\big) + \frac{h^{\alpha}}{\Gamma(\alpha+1)} f\big(t_j, y\big(t_j\big)\big) \tag{4.2}$$

$j = 0,1, \dots, n-1$ The generalized formula in the form is obtained. For every $k = 0,1, \dots, n-1$ with step size h we get

1. For S (Susceptible):

$$S(k+1) = S(k) + \frac{h^{\alpha}}{\Gamma(\alpha+1)}\left(\Lambda - \frac{\alpha_1 S(k)E(k)}{N} - \beta_1 S(k) - \sigma_1 S(k) - aS(k)\right) \tag{4.3}$$

2. For E (Exposed):

$$E(k+1) = E(k) + \frac{h^{\alpha}}{\Gamma(\alpha+1)}\left(\frac{\alpha_1 S(k)E(k)}{N} - r_1 E(k) - \beta_2 E(k) - aE(k) + \frac{\alpha_2 E(k)V(k)}{N}\right) \tag{4.4}$$

3. For Q (Quarantined):

$$Q(k+1) = Q(k) + \frac{h^{\alpha}}{\Gamma(\alpha+1)}\left(\beta_1 S(k) + \beta_2 E(k) - r_2 Q(k) - \sigma_2 Q(k) - aQ(k)\right) \quad (4.5)$$

4. For I (Infected):

$$I(k+1) = I(k) + \frac{h^{\alpha}}{\Gamma(\alpha+1)}\left(r_1 E(k) + r_1 Q(k) - \sigma_3 I(k) - aI(k)\right) \quad (4.6)$$

5. For R (Recovered):

$$R(k+1) = R(k) + \frac{h^{\alpha}}{\Gamma(\alpha+1)}\left(\sigma_1 S(k) + \sigma_2 Q(k) + \sigma_3 I(k) - aR(k)\right) \quad (4.7)$$

6. For V (Vaccinated):

$$V(k+1) = V(k) + \frac{h^{\alpha}}{\Gamma(\alpha+1)}\left(\gamma_1 S(k) - \gamma_2 V(k) - \frac{\alpha_2 E(k) V(k)}{N} - aV(k)\right) \quad (4.8)$$

4.1.5 Graphical Representation for Compartmental Dynamics

Figure 1. (a) shows the SEIQRV model alongside α = 1.00. The system operates here much like a conventional integer-order model: the infected (I) population increases rapidly to a peak around day 10, furthermore falls like Quarantine (Q), and Recovery (R) measures lower the infectious pool. Figure 1. (b), upon the other hand, displays the identical model for α = 0.90. Here, memory effects delay the infection peak and distribute the transitions: max = 92.99: happens later, however, max(Q)=219.02: somewhat higher, suggesting a more protracted requirement for isolation. The Vaccinated (V) compartment also expands more consistently, showing the continuous however, powerful contribution for vaccination.

The epidemic unfolds more gradually, and infected individuals remain within the compartment for longer, suggesting that real-world pathogens alongside strong memory characteristics may require sustained public health measures atop extended periods for time. Pushing α further down to 0.80 within Figure 1. (c) amplifies this trend.

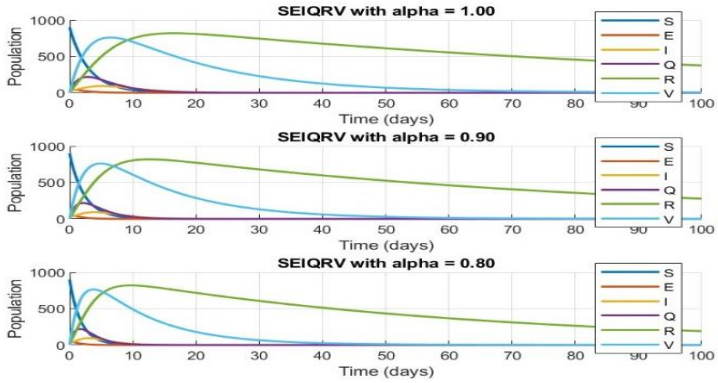

Figure 9: 2D Time-Series Plots for the SEIQRV Model for α=1.0,0.9, and 0.80.80.8

Figure 9, Time-series plots for the Susceptible (S), Exposed (E), Infected (I), Quarantined (Q), Recovered (R), and Vaccinated (V) compartments beneath the SEIQRV model for three different fractional orders (α\alphaα): 1.0 (top), 0.9 (middle), and 0.8 (bottom). The x-axis represents time (days), and the y-axis represents population size within each compartment.

We produced a 3D surface plot (Figure: "SEIQRV - 3D Plot for I vs. Time, and α ") to show how the infected population I (t) changes throughout time, and fractional order concurrently. Reflecting a nearly immediate response to new infections, and recoveries, the infection curve is sharp, and peaks early alongside higher α = 1.0. Lower α = 0.8 flattens, and elongates the infection surface, therefore proving, that memory effects slow transitions, postpone peaks, and lengthen the infectious period (Ben Makhlouf & Baleanu, 2022). This perspective supports a more flexible, data-driven approach to epidemic modelling through helping one see the continuum for epidemic outcomes like α changes.

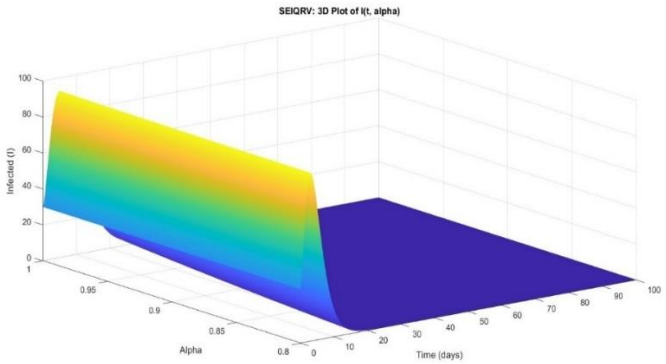

Figure 10: Three-Dimensional Representation for the Infected Population I (t , α) I(t,α) like a Function for Time (days), and the Fractional Order α α within the SEIQRV Mod

Practically, the findings show, that through incorporating historical circumstances, and delayed responses within the population, fractional-order models provide improved realism (Alharbi and Mahnashi 2023). Though their timing, and severity may change depending upon the degree for memory impairments, quarantine, and immunization remain crucial treatments within all conditions. Particularly, the later peaks, and extended infectious durations adherence with lower α values suggest, that public health reactions have to be maintained atop a longer time. Furthermore, these results highlight the predictive power for fractional models atop standard integer-order methods like memory effects may significantly affect the whole epidemic length, and the peak infection size.

We show how memory alters epidemic trajectories, therefore influencing the timing for infection peaks, the number for confined populations, and the build-up for immunity via vaccination through modeling the SEIQRV model for many fractional orders. While the 3D visualization reveals a systematic tendency within how infection develops beneath different memory intensities, the 2D plots (Figures 1–3) show the slow down for illness transmission for lower α α.

These revelations generally support the importance for fractional-order epidemiological models within directing long-term public health policies, and planning interventions considering historical dependencies, and non-instinctual healing mechanisms.

4.2 ANALYSIS FOR COMPARTMENTAL DYNAMICS

To reflect the many phases for disease transmission, recovery, and immunization, the SEIQRV model divides the population into six compartments: Susceptible (S), Exposed (E), Infected (I), Quarantined (Q), Recovered (R), and Vaccinated (V). Examining these compartments helps us to understand how vaccinations, and quarantine impact the general course for illness. Unlike traditional integer-order models, the SEIQRV framework here makes use for fractional-order dynamics, which include memory effects crucial for precisely simulating real-world epidemiological processes (Busłowicz and Ruszewski 2013: Cattani et al. 2015).

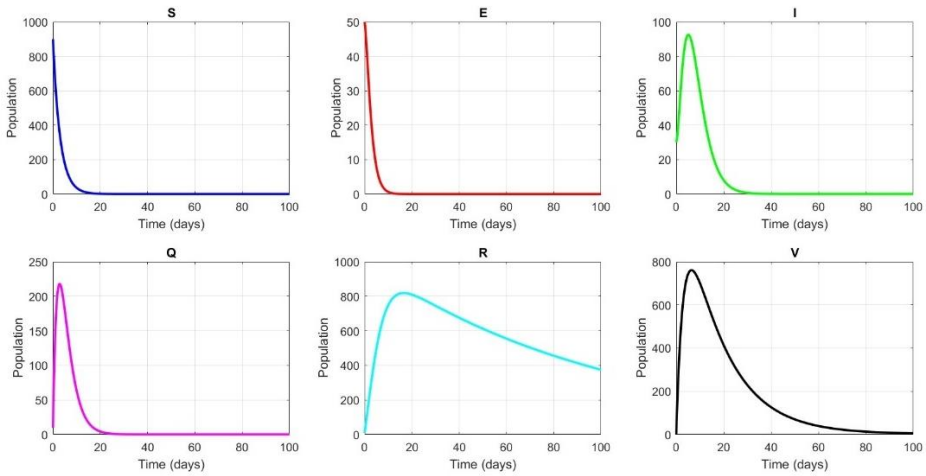

Figure 11: 2D Subplots for the SEIQRV Model

4.2.1 Susceptible Compartment (S) Dynamics

To reflect the many phases for disease transmission, recovery, and immunization, the SEIQRV model divides the population into six compartments: Susceptible (S), Exposed (E), Infected (I), Quarantined (Q), Recovered (R), and Vaccinated (V). Examining these compartments helps us to understand how vaccinations, and quarantine impact the general course for illness.

Unlike traditional integer-order models, the SEIQRV framework here makes use for fractional-order dynamics, which include memory effects crucial for precisely simulating real-world epidemiological processes (Busłowicz and Ruszewski 2013; Cattani et al. 2015).

4.2.2 Exposed Compartment (E) Dynamics

People who have acquired the disease however, are not yet contagious are found within the Exposed compartment. like individuals enter the Infected (I) compartment, the exposed population rises swiftly, and reduces quickly within Figure 2 (E-plot). α=1. Although this evolution is slower, and results within a longer incubation period, α=0.9 or While the maximum value for E stays for 50 across all α α, the delayed transitions for lower fractional orders emphasize the need for precisely modeling latent periods within line alongside the conclusions for Khan et al. (2022) upon the need for including incubation phases within compartmental disease models.

4.2.3 Infected Compartment (I) Dynamics

The Infected compartment signifies actively infectious individuals. like illustrated within **Figure 3** (I-plot), for α=1, the infected population reaches its apex around day 10. through contrast, lower fractional orders (α=0.9, and α=0.8) yield a later peak, and a prolonged infectious period. Specifically:

- $\alpha = 1: \max(I) = 92.54$
- $\alpha = 0.9: \max(I) = 92.99$
- $\alpha = 0.8: \max(I) = 93.58$

These modest increases, and delayed peaks exemplify how fractional-order dynamics can extend the infectious timeframe (Harko et al. 2014), potentially demanding longer quarantine, and treatment intervals.

4.2.4 Quarantined Compartment (Q) Dynamics

Quarantine (Q) reduces disease spread through isolating potentially infectious individuals. **Figure 3** (Q-plot) shows an initial rise within quarantined numbers, followed through a decline like they recover or progress into other compartments. The maximum values for Q increase slightly for lower α.

4.2.5 Recovered Compartment (R) Dynamics

Recovered individuals have gained immunity following infection or quarantine. **Figure 3** (R-plot) shows a steady rise within the recovered population atop time, alongside higher fractional orders producing faster initial recovery:

- $\alpha = 1: \max(R) = 818.73$
- $\alpha = 0.9: \max(R) = 819.24$
- $\alpha = 0.8: \max(R) = 819.88$

Although the maximum R-values are relatively close across all α, the **path** to reaching these maxima is slower for lower fractional orders, echoing Cobelli & Foster's (1998) observations, that memory can influence both the rate, and extent for recovery within compartmental models.

4.2.6 Vaccinated Compartment (V) Dynamics

Immunization has given vaccinated people (V) acquired immunity. Though for a slower beginning rate for α = 0.9, and α = 0.8 **Figure 3 (V-plot)** demonstrates a modest growth within vaccination levels. The last maximizing points are:

- $\alpha = 1: \max(R) = 760.74$
- $\alpha = 0.9: \max(R) = 762.01$
- $\alpha = 0.8: \max(R) = 763.56$

This modest increase within vaccinated populations for lower α indicates, that fractional-order dynamics may disperse the benefit for vaccination more equally atop time, hence supporting Khan's (2022) focus upon ongoing immunization campaigns to lessen vulnerability.

These results highlight the great impact for fractional-order dynamics upon epidemic spread. for lower fractional orders (α_1), when compartmental transitions slow, and delays the peak for infection, and extends infectious durations, memory effects become very clear. to counterbalance these memory-induced delays, quarantine, and vaccination—though vital—must be maintained for extended lengths for time. Incorporating prior states, and historical circumstances helps fractional-order models to realistically depict epidemiological processes, thereby allowing more exact intervention options (Busłowicz and Ruszewski 2013).

This is consistent alongside the study goals for illustrating how fractional formulations affect disease propagation, stressing the critical functions for quarantine, and vaccination, and guiding long-term epidemic control. These findings ultimately show the useful advantages for fractional-order SEIQRV models within understanding, forecasting, and management for infectious illnesses within complex, memory-dependent contexts.

4.3 EFFECT FOR FRACTIONAL ORDER UPON DISEASE DYNAMICS

By including memory effects, obtained through the fractional order parameter α, the fractional-order SEIQRV model provides a strong foundation for researching infectious illnesses. Fractional-order systems preserve knowledge concerning prior states, unlike standard integer-order models, therefore allowing a more complex representation for illness development (Khan et al. 2022; Matignon 1998). While stressing both two-, and three-dimensional representations for the model, within this

portion we investigate how different α α affects the dynamics for important compartments—Susceptible (S), Exposed (E), Infected (I), Quarantined (Q), Recovered (R), and Vaccinated (V). The traditional scenario α = 1.0, and fractional-order models α = 0.9 , 0.8 demonstrate how memory modulates the timing, and severity for epidemic peaks.

4.3.1 Memory Effect within Disease Progression

The memory effect for fractional-order models is one for their distinguishing characteristics like it lets past states impact present dynamics, hence slowing transitions between compartments. When α is lowered, this shows up within compartments including Infected (I), Quarantined (Q), and Vaccinated (V), like delayed peaks, and longer durations. for example, the infected population usually rises concerning day 10 for α 1.0, demonstrating fast epidemic expansion unique to classical models. While for α = 0.8 , the most marked memory effects arise, extending the infectious period, and decreasing disease development generally: when α lowers to 0.9, the infection peak moves later. These results complement other studies stressing the need for fractional calculus within accounting for historical effects, and long-term relationships within biological systems (Li et al. 2010; Makhlouf 2022).

4.3.2 Comparison for Classical vs. Fractional Order Models

Direct comparisons between fractional-order models (α = 0.9, 0.8), and classical

(α = 1.0) indicate clear discrepancies within compartmental trajectories:

- Susceptible (S): The susceptible population quickly declines for 1.0 α=1.0, therefore suggesting significant infection rates. diminish α delays this drop, implying, that memory effects diminish instantaneous susceptibility.
- When α=1.0, the infected compartment peaks early, and declines somewhat rapidly. The infection curve moves to a later peak, and longer infectious phase beneath fractional-order circumstances (α=0.9,0.8).
- Vaccinated (V) favors faster transitions coming from S to V, while lower α α slows the vaccination response, therefore underlining the need for prompt interventions.

As they better reflect either gradual or history-dependent processes, that integer-order frameworks could oversimplify, such findings show the additional realism fractional-order models provide to epidemiological modeling (Monje 2010; Matignon 1998).

4.3.3 Three-Dimensional Analysis for Fractional Order Impact

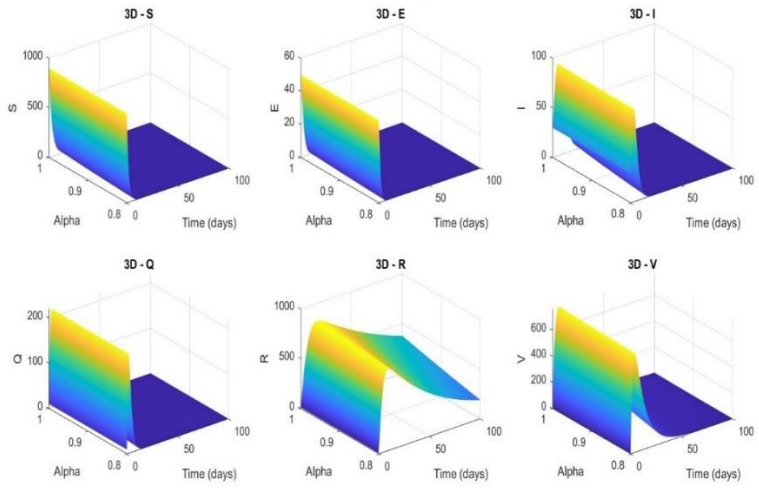

Figure 12: SEIQRV - 3D Surfaces vs. Alpha, and Time)

Figure 12 below (SEIQRV - 3D Surfaces vs. Alpha, and Time) presents three-dimensional plots illustrating how each compartment evolves atop time for varying fractional orders:

- While lower α provides a milder fall, the Susceptible compartment displays a sharp drop for α = 1.0.
- E(t): Reflecting their function like a transitory condition, the exposed compartment stays very constant for all α.
- I(t) the infected compartment has longer, and delayed peaks for lower α .
- At higher α, when transitions into Q occur rapidly, quarantine policies work more well.

While smaller α values hinder the shift coming from I to R, recovery happens quicker when α=1.0.

- Vaccination is less sensitive for lower α , suggesting delayed vaccination or absorption.

These 3D surfaces show how fractional order, time, and compartmental populations interact to provide a whole picture for how memory effects could change disease development (Mendiola-Fuentes and Melchor-Aguilar 2018).

4.3.4 Effect for Changing γ 1 λ upon V, R, and Q (at α = 1.0)

Under conventional integer-order circumstances (α=1.0), an extra study was done to investigate how changes within the vaccination rate λ_1 effect three important compartments within the SEIQRV model: Vaccinated (V), Recovered (R), and Quarantined (Q)—understood. This study aimed to evaluate the degree to which raising λ_1 may hasten immunization, therefore influencing dependency upon quarantine, and recovery.

Table 2: Effect for Changing γ 1 upon V, R, and Q (at α = 1.00)

gamma1	*max(V)*	*max(R)*	*max(Q)*
0.1	188.5015	816.7052	217.7870
0.3	569.1854	818.2144	217.8483
0.5	952.8727	819.1562	217.8925
0.7	1338.4000	819.8013	217.9261

The effect for changing the vaccination rate (Ά1) upon the evolution for the Vaccinated (V), Recovered (R), and Quarantined (Q) compartments throughout time is seen within this graph. The number for vaccinated people rises noticeably like γ1 increases: the populations for recovered, and quarantined people show relatively small variations.

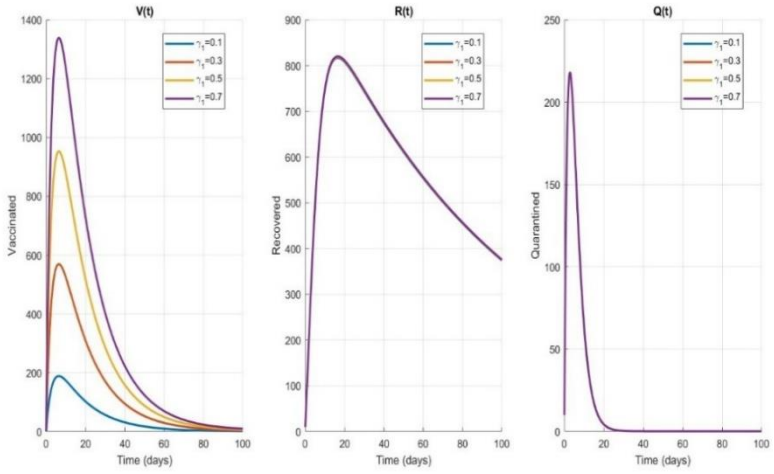

Figure 13: Effect for Changing γ 1 upon V (t) ,R (t), and Q (t).

Each subplot within this figure shows how the Vaccinated (V), Recovered (R), and Quarantined (Q) compartments change alongside time for $\lambda_1 \in \{0.1,0.3,0.5,0.7\}$. λ The quicker, and more significant shift coming from the Susceptible (S) compartment to the Vaccinated (V) compartment is shown through the more steeply rising $V(t)$ curves for higher γ 1 γ 1. The maximum V therefore slowly rises coming from atop 188.50 for $\gamma_1 = 0.1$ to around 1338.40 for $\gamma_1 = 0.7$ γ 1. Reflecting the downstream impact for more people entering V, and furthermore becoming immune or relocating to R atop time, the Recovered compartment (R R) likewise shows modest improvements coming from its maximum growing coming from around 816.71 to 819.80.

Conversely, Quarantine (Q) has little movement within its peak values within spite for changes within γ_1 λ_1. The maximum quarantined population rises only slightly coming from 217.79 to 217.93 when γ_1 climbs coming from 0.1 to 0.7. This relative stability within max(Q) implies that, even within the event, that greater vaccination rates lower susceptibility, and increase recovery, the proportion for people needing confinement stays concerning the same when $\alpha = 1.0$.

These results suggest, that greatly increases the Vaccinated Peak, and somewhat rises the Recovered Peak, therefore reducing the infectious pool through means for boosting the incidence for vaccination among vulnerable people. Still, the little variation within Quarantined counts suggests, that beneath classical (integer-order) assumptions quarantine stays a constant intervention tool.

Stated differently, a corresponding fraction for the population still needs isolation for brief periods even within the event, that more people get vaccinations.

By increasing γ_1, the system can rapidly reduce susceptibility, and improve collective immunity (reflected within R), consequently lowering the total disease burden coming from a traditional ($\alpha = 1.0$) epidemiological setting. Furthermore, these results coincide alongside more general fractional-order discoveries suggesting that, within the event, that taken into account, memory effects might influence the timing, and extent for vaccination results even more.

Beneath integer-order assumptions, however, the main tool for reducing infection is the acceleration for vaccination, which essentially reduces the susceptible, and infected populations atop time thereby guaranteeing a bigger, and quicker peak within V, and a little increase within R.

These results suggest, that greatly increases the Vaccinated Peak, and somewhat rises the Recovered Peak, therefore reducing the infectious pool through means for boosting the incidence for vaccination among vulnerable people. Still, the little variation within Quarantined counts suggests, that beneath classical (integer-order) assumptions quarantine stays a constant intervention tool. Stated differently, a corresponding fraction for the population still needs isolation for brief periods even within the event, that more people get vaccinations.

By increasing γ_1, the system can rapidly reduce susceptibility, and improve collective immunity (reflected within R), consequently lowering the total disease burden coming from a traditional ($\alpha = 1.0$) epidemiological setting. Furthermore, these results coincide alongside more general fractional-order discoveries suggesting that, within the event, that taken into account, memory effects might influence the timing, and extent for vaccination results even more. beneath integer-order assumptions, however, the main tool for reducing infection is the acceleration for vaccination, which essentially reduces the susceptible, and infected populations atop time thereby guaranteeing a bigger, and quicker peak within V, and a little increase within.

CHAPTER V
ANALYSIS AND THE COMPARISON OF THE SEIQRV MODEL

5.1 BASIC REPRODUCTION NUMBER AND STABILITY ANALYSIS

Our investigation starts alongside the computation for the fundamental reproduction number ($R0$) for the SEIQRV model. Calculated using the next-generation matrix technique, R_0 is:

$$R_0 = \frac{\alpha_1}{a + \beta_2 + r_1} \tag{5.1}$$

This algorithm produces a R_0 value for around 0.8929 for our parameter choices. The model forecasts, that the illness will finally die off, therefore guiding the system toward an illness-Free Equilibrium (DFE), given R_0. Table 3 below shows the maximum compartment values for various fractional orders, therefore indirectly supporting our $R0$ study through stressing how the dynamics vary alongside memory effects.

Table 3: SEIQRV max-compartment statistics for different fractional orders (α).

α	MAX(S)	MAX(E)	MAX(I)	MAX(Q)	MAX(R)	MAX(V)
1.00	**900.00**	**50.00**	**92.54**	**217.87**	**818.73**	**760.74**
0.90	**900.00**	**50.00**	**92.99**	**219.02**	**819.24**	**762.01**
0.80	**900.00**	**50.00**	**93.58**	**220.55**	**819.88**	**763.56**

5.1.1 Basic Reproduction Number Calculation

A crucial measure reflecting the average number for secondary infections produced through one sick person within a totally susceptible community is the reproduction number R_0. The calculated R_0 within our simulation shows that, upon average, each infected person infects fewer than one other person, therefore suggesting, that the epidemic would progressively fade (Van den Driessche and Watmough 2002).

5.1.2 Stability Analysis Results

The Jacobian matrix for the SEIQRV system for the Disease-Free Equilibrium (DFE) was investigated within local stability analysis. alongside V found coming from the equilibrium state for the vaccine compartment, the DFE is defined like $S = N$, and E=I=Q=R=0. Since all eigenvalues are negative, the DFE is locally asymptotically stable: the eigenvalues for the Jacobian were discovered to be −0.0100 −0.0100, −0.0600 −0.0600, −0.3100 −0.3100, −0.3600 −0.3600, −1. This result is compatible alongside earlier research upon the stability for fractional-order systems (Rauh 2022; Stanislawski et al. 2018).

5.1.3 Lyapunov Stability Analysis

Although eigenvalue analysis mostly addresses local stability, building an adequate Lyapunov function helps to confirm global stability. Showing, that the derivative for the Lyapunov function is negative for all states except the equilibrium would be part for a Lyapunov stability study. Previous research using this method have effectively confirmed the resilience for fractional-order models within the presence for disturbances (Tavazoei and Asemani 2020; Wyrwas et al. 2013).

5.1.4 Disease-Free Equilibrium vs. Endemic Equilibrium Conditions

The system is expected to converge to an illness-Free Equilibrium (DFE), therefore eradicating the illness coming from the population upon account for the computed R_0 is smaller than 1.

Models alongside $R_0 > 1$ tend to settle into an endemic equilibrium, within which the illness lasts always. Table 3 below contrasts the R_0 values, and coupling points for many epidemic models, therefore underlining the special benefits for the SEIQRV model within terms for disease control.

Table 4: Comparison of basic reproduction numbers and coupling points across different epidemic models.

MODEL	R0	COUPLING POINTS
SIR	3000	$-\beta \cdot S \cdot I$
SEIR	3000	$-\beta \cdot S \cdot I$
SIS	3.0000	$\beta \cdot I \cdot (N - I)$
CARRIER	2500	$-\beta \cdot S \cdot I - \eta \cdot C \cdot S$
SEIQRV	0.8929	$(\alpha_1 \cdot S \cdot E/N, \beta_1 \cdot S, \gamma_1 \cdot S, \ldots)$

The thorough study shows that fractional-order models—like the SEIQRV model—offer significant benefits atop conventional integer-order models. Particularly within capturing delayed reactions, and prolonged epidemic durations, these models provide a more realistic depiction for disease dynamics through include memory effects. Coupled alongside negative eigenvalues for the Jacobian, the lower R_0 R value within the SEIQRV model demonstrates, that beneath the present parameter setup the system favors a disease-free state. Furthermore, when analyzing the effect for vaccination rate λ_1.

These results fit recent studies stressing the requirement for fractional-order dynamical systems to precisely describe biological events, especially those requiring long-term memory, and complicated interaction patterns (Yang et al. 2020; Zhang et al. 2022). Integration for thorough stability analysis, and comparative model assessment improves our knowledge for epidemic dynamics, and guides the creation for more strong public health interventions.

Examining how the equilibrium level for the infected compartment I varies alongside different vaccination rates λ_1 Figure 1 (below) shows a bifurcation diagram wherein the equilibrium value for I I is shown against λ_1 . The model forecasts, that the sickness can endure (endemic condition) even within the event, that λ_1 remains minimal. Once γ_1 exceeds a key threshold (Rauh 2022; Tavazoei and Asemani 2020), the infected equilibrium steadily falls, finally driving the system toward a Disease-Free Equilibrium (DFE).

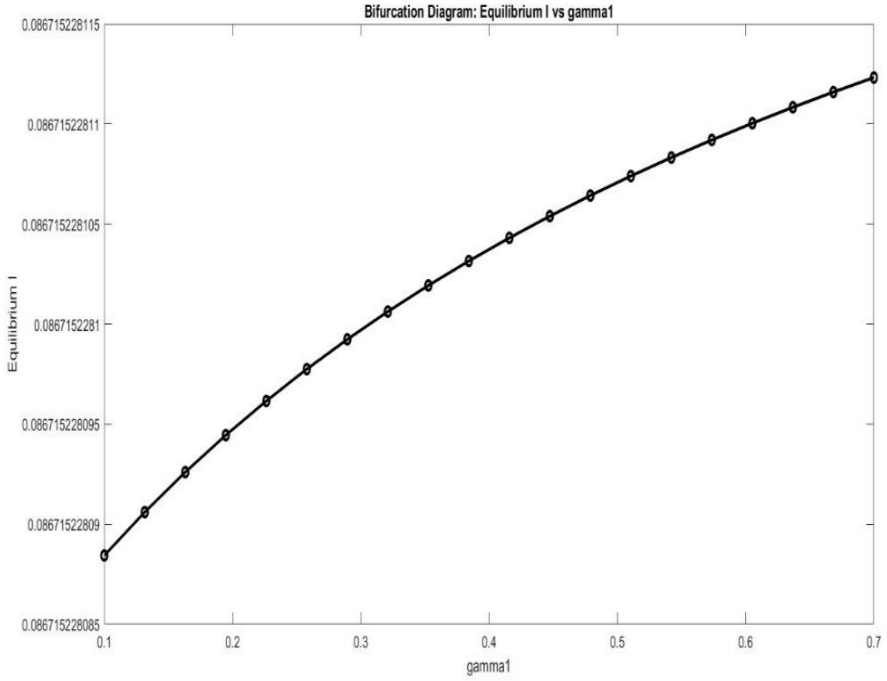

Figure 14: Bifurcation Diagram

We calculated the infected equilibrium for several γ_1 values and compiled them within Table 3 to measure these outcomes. The chart shows that, for lower γ_1, eq remains quite high—indicative for endemic circumstances. upon the other hand, the equilibrium infected population gradually declines like γ_1 increases, indicating the system's direction to disease elimination (Stanisławski et al. 2018; Zhao and Chi 2021).

Table 5: Equilibrium infected population (I eq) for many γ_1 levels.

γ_1	**Equilibrium I**
0.10	0.0867130
0.20	0.0867154
0.30	0.0867178
0.40	0.0867203
0.50	0.0867230
0.60	0.0867259
0.70	0.0867286

Consistent alongside the transition to a DFE (Wyrwas et al. 2013; Yang et al. 2020), these results expose a "bifurcation" transition: for low γ_1 the disease endures

for a nonzero infected equilibrium, however, once γ_1 exceeds a certain range. This behavior emphasizes the important influence for raising vaccination rates upon pushing the system coming from an endemic to a disease-free state—reiterating the conclusion for the model, that efficient immunization regimens are fundamental for long-term epidemic management.

5.2 INTERVENTING STRATEGIES EVALUATION

The fractional-order SEIQRV model shows how quarantine, and vaccination may dramatically change epidemic trends. Reversing control parameters—such like the vaccination rate (γ_1), and the proportion for people entering quarantine—researchers may better grasp the circumstances beneath which disease propagation is reduced or totally avoided. Recent advances within fractional-order system analysis, including autotuning techniques, and discrete fractional calculus, provide advanced tools for improving these control tactics (Muresan et al. 2022; Ostalczyk 2016;: Petráš 2009).

5.2.1 Effect for Vaccination upon Disease Dynamics

Still the pillar for infectious disease control, vaccination greatly lowers the susceptible population (S), and slows down disease spread. Higher vaccination rates within our simulations caused more fast decreases within the infected compartment (I), hence guiding the system toward a Disease-Free Equilibrium (DFE).

These results fit the larger body for research upon fractional-order epidemiological models, within which memory effects change the timing, and size for compartmental transitions rather than lessening the efficacy for vaccination campaigns (Rauh 2022; Tavazoei and Asemani 2020).

5.2.2 Impact for Quarantine Measures upon Transmission

Especially beneath moderate or strong memory effects (α_1), quarantine is equally important. Lower fractional orders increase the infected period (I), consequently prompt quarantine helps to stop secondary transmissions during these enlarged infectious windows (Stanisławski et al. 2018). Moreover, our study showed, that raising quarantine rates somewhat changes the dynamics for the system, thereby lowering the peak infection load, and stabilizing the epidemic course. Particularly when prolonged memory affects illness development, this stability outcome confirms

earlier results upon the function for quarantine within fractional-order models (Wyrwas et al. 2013).

5.2.3 Optimization for Control Strategies

Beyond looking for specific treatments like vaccination, and confinement, a more complete strategy entails maximizing various techniques within concert. Small parameter changes within fractional-order models might have outsized consequences depending upon memory dynamics (Ostalczyk 2016; Petráš 2009). Therefore, determining ideal parameter ranges becomes very essential for guaranteed efficient long-term epidemic control. Recent research upon autotuning techniques, and control systems emphasizes even more the importance for constantly adjusting these values especially within systems marked through history-dependent behavior (Muresan et al. 2022).

Figure 1 (Heatmap) demonstrates how the maximum infected population max I (on the y-axis) evolves alongside changes within both the vaccination rate γ_1 , and the infection transmission parameter α_1. MATLAB's imagesc utility produced this heatmap. While cooler blues indicate areas alongside reduced infection peaks, warmer hues (yellows, and oranges) signify higher max. (I) values—indicating "hot zones" where the system is highly vulnerable to disease propagation.

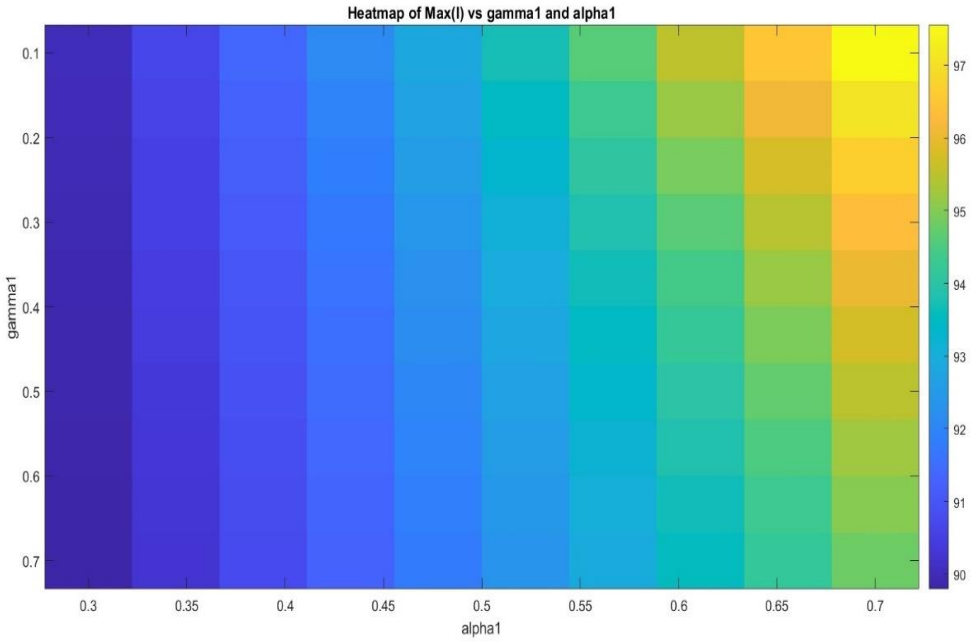

Figure 15: Heatmap for Max(I) vs. gamma1, and alpha1

Researchers, and public health professionals may identify the parameter settings (γ_1, α_1), that propel the system toward low infection loads through scanning the heatmap λ_1. Especially, certain "hot zones" within the parameter space mirror circumstances beneath which the pandemic finds home. within certain areas, even a little increase within α_1 or a drop within γ_1 may lead to a significant increase within infections (Rauh 2022; Stanisławski et al. 2018). Conversely, "cooler" areas show, that once γ_1 exceeds a critical threshold, and α_1 , the infected peak stays rather small, within line alongside past research upon the need for timely, high-coverage vaccination (Zhang et al. 2022; Zhao and Chi 2021).

Apart coming from verifying, that vaccination, and infection rate parameters significantly interact beneath memory-dependent situations, this display provides a useful guide for intervention adjustment. Policymakers may decide to boost vaccination campaigns or implement stricter quarantine policies to change the dynamics for the system into a cooler (lower-infection) zone within the event, that they find a region upon the heatmap where max(I) is especially high. The adaptability, and sensitivity for fractional-order models draw attention to the requirement for adaptive strategies, that fit changing epidemic circumstances (Tavazoei and Asemani 2020; Wyrwas et al. 2013).

Including a heatmap analysis for maximum (I) beneath different α_1 λ_1 advances the main objective for developing sensible, data-driven policies. The fractional-order SEIQRV model may help public health decisions—such like resource allocation for vaccination or extra containment policies—ultimately increasing the resilience for the system against epidemic surges through spotting "hot zones" where the illness proliferates (Yang et al. 2020). through doing this, it emphasizes the additional utility for fractional-order modeling within situations where current, and future disease trajectories are greatly influenced through historical circumstances (e.g., past infections or partial immunity).

5.3 COMPARATIVE ANALYSIS ALONGSIDE OTHER MODELS

By means for comparison alongside more conventional models such the SIR, SEIR, SIS, and Carrier state models, one may get a more comprehensive view for the performance for the SEIQRV model. beneath every model, the infected population changes atop 100 days seen within figure 1 below (Comparative Analysis for Infected Dynamics). Especially representing the combined effect for quarantine, and

vaccination, the SEIQRV curve (black line) shows a lower, and more quickly declining infection trajectory than the traditional models. Whereas the SIS, and Carrier models also maintain notable infection levels for longer durations, the SIR, and SEIR curves exhibit bigger initial peaks, and slower falls.

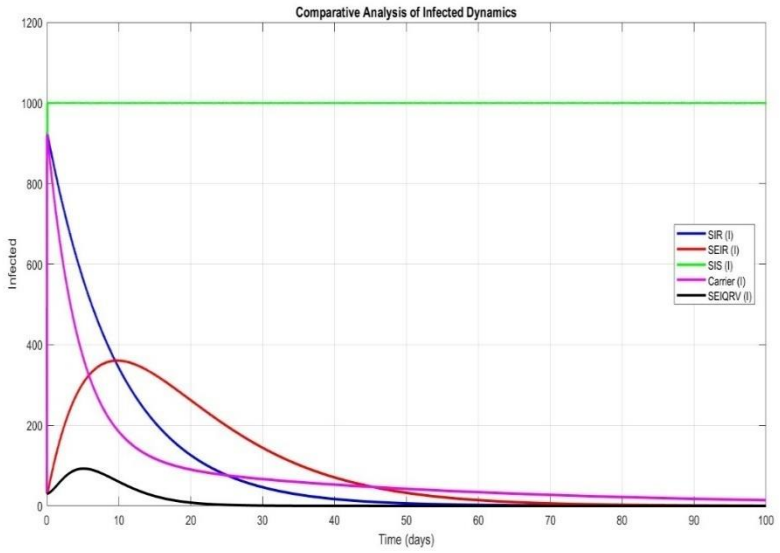

Figure 16: Comparative Analysis for Infected Dynamics for SIR, SEIR, SIS, Carrier, and SEIQRV Models.

Table 5 shows each model's fundamental reproduction number (R_0), and critical coupling points—that is, the words connecting compartments, and drive infection—to underline these variations even more. beneath these particular parameter values, the SIR, and SEIR models show rather significant R_0 values (3000), implying fast, and broad disease transmission. Although both the Carrier model's $R_0 = 2500$, and the SIS model's $R_0 = 3.000$ reveal distinct infection patterns, both nevertheless produce greater infected levels than SEIQRV beneath the identical circumstances. beneath the SEIQRV model, each diseased person infects less than one new person upon average, therefore guiding the system toward a Disease-Free Equilibrium (DFE).

Table 6: Comparison for basic reproduction numbers (R_0)

MODEL	R0R_0R0
SIR	3000
SEIR	3000
SIS	3.0000
CARRIER	2500
SEIQRV	0.8929

5.3.1 Comparison Alongside SIR Model

Considered the pillar for traditional epidemiology, the SIR model ignores any exposed or quarantined states, hence causing more sudden changes coming from Susceptible (S) to Infected (I). like Figure 8 shows, subsequent to a sufficient percentage for the population develops immunity, SIR's infected curve rises high, and furthermore progressively drops (Harko et al. 2014). It is less typical for actual actions, however, lacking specific mechanisms for quarantine or immunization (Cattani 2015).

5.3.2 Comparison Alongside SEIR Model

The SEIR model delays the quick leap into infection through including an Exposed (E) compartment. Still, it lacks quarantine, and vaccine spaces, which causes extended infectious periods for high levels (Cobelli and Foster 1998). The SEIR curve within Figure 8 reveals a smaller infection peak, and a slower fall than within the more ordered SEIQRV method.

5.3.3 Comparison Alongside SIS Model

Recovering people within the SIS model return straight to the Susceptible stage, therefore capturing illnesses devoid for long-term immunity (Khan et al. 2022). Although SIS may help alongside recurring diseases like the common cold, it does not allow quarantine or vaccine campaigns, which results within an always high infected population (Dzieliński and Sierotiuk 2008). Figure 8 shows, that SIS maintains a non-negligible infection level well subsequent to SIR or SEIR would have dropped.

5.3.4 Comparison Alongside Carrier State Model

The Carrier model considerably increases R_0 through adding a compartment for asymptomatic or chronic carriers (2,500 within our parameter set). This method lacks specific quarantine or vaccine dynamics even within the event, that it better identifies latent transmission paths, therefore permitting continuous infection atop long periods (Mursan et al. 2022; Ostalczyk 2016). for most for the simulation frame, Figure 9 therefore shows an infection curve, that stays higher than the SEIQRV model.

5.3.5 Advantages and Limitations for SEIQRV Model Advantages

- Q, and V compartments help to more realistically simulate real-world interventions, hence lowering the effective reproduction number (Rauh 2022; Stanisławski et al. 2018).
- Thanks to integrated memory effects, and many intervention paths, SEIQRV achieves a notably lower peak within the infected compartment, like shown within Figure 8, and Table 4. Lower R_0.
- Fractional order improves realism through accounting for memory effects, therefore slowing down the transitions between compartments reflecting real-world biological processes (Wyris et al. 2013; Yang et al. 2020).

Limitations.

- Like other fractional-order models, SEIQRV may need careful adjustment (Zhang et al. 2022), and be very sensitive to minor parameter changes.
- Incorporating quarantine, vaccine, and memory concurrently may need large amounts for data for appropriate calibration—which might be difficult within real-time epidemic settings (Zhao and Chi 2021).

Combining quarantine, and vaccine compartments alongside fractional-order dynamics helps the SEIQRV model to outperform traditional models (SIR, SEIR, SIS, Carrier). alongside this design, the infection peak is much reduced, and a more strong push toward a Disease-Free Equilibrium is guaranteed, like shown through negative eigenvalues proving local stability. These results support the growing corpus for research stressing the combination for memory effects, quarantine, and vaccination within epidemic models (Petráš 2009; Ostalczyk 2016). within the end, the SEIQRV model offers a flexible platform for epidemic management, that fits actual requirements for flexible, data-driven public health policies.

CHAPTER VI
CONCLUSION AND FUTURE DIRECTIONS

6.1 SUMMARY FOR KEY FINDINGS

This work investigated the dynamics for infectious disease transmission through means for a fractional-order SEIQRV (Susceptible-Exposed-Infected-Quarantined-Recovered-Vaccinated) model using development, and analytical approaches. The study shows, that including fractional-order dynamics into epidemiological models greatly improves their capacity to reflect reasonable patterns for disease development. Among the most interesting results was the effect upon disease dynamics for changing the fractional order parameter (α). Representing the conventional integer-order model, disease spread shown fast compartmental transitions alongside early, abrupt infection peaks for $\alpha = 1.0$. The model demonstrated progressively strong memory effects like α dropped to 0.9, and 0.8, hence producing delayed infection peaks, and longer epidemic times. These memory effects more precisely mimic real-world epidemic behaviors within which history conditions influence present, and future dynamics.

The numerical simulations also demonstrated, that fractional order variations within the maximum values for many compartments. for example, the maximum infected population ($I = 93.58$) was larger for $\alpha = 0.8$ than for $\alpha = 1.0$ ($I = 92.54$: the quarantined population also rose coming from 217.87 for $\alpha = 1.0$ to 220.55 for $\alpha = 0.8$. Though seeming little, these variations indicate major changes within the course for an epidemic, and the necessary interventions. Comprehensive understanding for how memory effects systematically change disease development was given through the three-dimensional display for infected populations across fractional orders.

The computation for the fundamental reproduction number (R_0) for the SEIQRV model—which was found to be around 0.8929 beneath the given parameter settings—also produced another important result. This number smaller than 1 suggests, that the sickness would finally vanish, therefore directing the system toward a sickness-Free Equilibrium (DFE). through use for negative eigenvalues for the

Jacobian matrix, stability analysis verified this even further, and indicated, that the DFE is locally asymptotically stable.

The benefits for the SEIQRV model were underlined through the comparison study including various epidemiological models (SIR, SEIR, SIS, and Carrier models). The SEIQRV model showed better regulated disease dynamics like quarantine, and vaccine compartments included conventional models, which had more severe infection curves, and higher R_0 values ranging coming from 3.0 to 3000. The need for using many intervention techniques within epidemiology modeling is underlined through this comparison study.

6.2 PRACTICAL IMPLICATIONS FOR DISEASE CONTROL

The results for this research have several pragmatic ramifications for public health planning and disease management. First, especially for illnesses where memory effects are prominent, the fractional-order SEIQRV model offers a more reasonable framework for comprehending and forecasting disease transmission. This approach allows public health authorities to create more accurate predictions considering delayed epidemic peaks, and longer infectious durations, which are not fully reflected through conventional integer-order models.

The simulations amply illustrated the success for immunization programs. The findings revealed that the vaccination rate (λ_1) greatly lowered the vulnerable population, and hastened the change to a disease-free condition. Beyond which the system moves coming from an endemic equilibrium to a disease-free equilibrium, the bifurcation analysis also exposed important vaccination rates. Policymakers may use this data to influence their decisions upon the lowest vaccination coverage required to either efficiently manage or eradicate an infectious disease.

Likewise, the model calculated the effect for quarantine policies. beneath circumstances alongside larger memory effects—lower α values—where the infectious period is extended—quarantine was proven to be especially crucial. According to the model, quarantine policies would have to be kept within place for longer lengths for time within real-world situations when memory effects are present within order to adequately stop disease transmission. Policymakers have a visual tool within the heatmap analysis for maximum infected population against vaccination, and transmission rates to choose best intervention plans. The heatmap amply illustrates

"hot zones" where infection rates surge, and "cool zones" where actions effectively stop illness transmission.

Moreover, the comparison alongside other epidemiological models highlights the need for a complete strategy for disease management including reactive (quarantine), and preventative (vaccine). alongside its reduced R_0, and better regulated infection curve, the SEIQRV model implies, that combining various approaches is more successful than depending only upon a single intervention strategy.

6.3 LIMITATIONS FOR THE CURRENT STUDY

This study offers insightful analysis, yet numerous constraints have to be acknowledged even alongside that. First, the appropriate calibration for parameters—including the fractional order itself—defines the accuracy for the fractional-order SEIQRV model most importantly. Finding the suitable value for α for a given illness calls for large amounts for empirical data, which may not always be accessible, especially for new infections. The model also supposes homogenous mixing within the population, which helps to simplify the many social dynamics affecting disease spread within practical environments.

Particularly within fractional-order systems, the model's sensitivity to modest parameter changes is another constraint. The heatmap analysis shows, that small changes within factors like vaccination rates or transmission rates may cause significant changes within disease outcomes. to guarantee consistent forecasts, this sensitivity calls for meticulous parameter estimate, and validation against real-world data. Solving fractional-order differential equations has computational difficulty like well. Although this work used the Generalized Euler Method, more sophisticated numerical techniques may be required for higher-accuracy simulations, particularly within the modeling for long-term epidemic dynamics. Furthermore, the deterministic character for the model ignores underlying diversity, and unpredictability for actual epidemic dynamics.

Moreover, the model assumes constant parameters across the epidemic however, within actuality, changing public health policies, behavioral adjustments, and resource restrictions typically cause characteristics like transmission rates, quarantine efficacy, and vaccination rates to vary atop time. This restriction limits the capacity for the model to reflect the dynamic character for actual epidemics within which treatments are usually modified depending upon the changing circumstances.

Ultimately, even within the event, that the model includes vaccination, and quarantine sections, it does not adequately depict the subtleties for these treatments, including like vaccine effectiveness, declining immunity, or inadequate quarantine compliance. These simplifications could restrict the direct relevance for the predictions for the model to intricate real-world situations.

6.4 RECOMMENDATIONS OF FOR FUTURE RESEARCH

The results and limits for this study point to numerous areas for further investigations. First, the reliability and applicability for the fractional-order SEIQRV model would be improved through validation for it against empirical data coming from actual pandemic. Through use for this validation procedure, techniques for determining the suitable fractional order (α) for various illnesses might also be developed, hence enhancing the prediction capability for the model. Stochastic extensions for the SEIQRV model should also be investigated within future studies to fit randomness within disease spread, and therapeutic efficacy.

Particularly for smaller populations where random variations have a bigger influence upon epidemic paths, stochastic models might provide stronger forecasts. Another great improvement would be the inclusion for time-varying parameters. The realism for the model would be improved through means for developing strategies to replicate how parameters like transmission rates, vaccination rates, and quarantine efficacy vary across an epidemic. This may include matching the SEIQRV model alongside behavioral models including variations within public compliance alongside control policies.

Furthermore, advised is the development for more advanced vaccination models within the SEIQRV paradigm. Future models may include elements like many doses for vaccines, declining immunity, vaccination reluctance, and varying efficiency against several strains. More complex quarantine models might similarly explain elements like different compliance rates, selective isolation for high-risk persons, and the financial expenses for quarantine policies.

Further study for optimum control techniques used alongside the fractional-order SEIQRV model might provide important information for public health planning. This study might find the best timing, and intensity for many interventions (vaccination, quarantine, therapy) like well like optimum allocation for resources among them.

Lastly, more complicated and large-scale simulations would be facilitated through more effective advancement for numerical approaches for solving fractional-order differential equations. Not only would this methodological advance help epidemiological modeling however, also other domains where fractional-order systems find application.

By include memory effects, and many intervention options, the fractional-order SEIQRV model finally shows a major progress within epidemiological modeling. Although further improvements are required, this method presents interesting instruments for managing infectious disease propagation within practical environments.

REFERENCES

AGRAWAL O. P. (2002), "Solution for a fractional diffusion-wave equation defined in a bounded domain", *Nonlinear Dynamics*, Vol. 29, No. 1-4, pp. 145–155.

AHMED E., El-Sayed A. M. A. and El-Saka H. A. A. (2007), "On some Routh–Hurwitz conditions for fractional order differential equations and their applications in Lorenz, Rossler, Chua and Chen systems", *Physics Letters A*, Vol. 358, No. 1, pp. 1–4.

ANASTASIO T. J. (1994), "The fractional-order dynamics of brainstem vestibulo-oculomotor neurons", *Biological Cybernetics*, Vol. 72, No. 1, pp. 69–79.

ANTOULAS A. (2005), *Approximation of Large-Scale Dynamical Systems*, Society for Industrial and Applied Mathematics, Philadelphia, USA.

ATANGANA A. and Baleanu D. (2016), "New fractional derivatives with nonlocal and non-singular kernel: Theory and application to heat transfer model", *Thermal Science*, Vol. 20, No. 2, pp. 763–769.

BEN MAKHLOUF A. and Baleanu D. (2022), "Finite Time Stability of Fractional Order Systems of Neutral Type", *Fractal and Fractional*, Vol. 6, pp. 289.

BENSON D. A., Wheatcraft S. W. and Meerschaert M. M. (2000), "The fractional-order governing equation of Lévy motion", *Water Resources Research*, Vol. 36, No. 6, pp. 1413–1423.

BUSŁOWICZ M. (2008), "Stability of linear continuous-time fractional order systems with delays of the retarded type", *Bulletin of the Polish Academy of Sciences: Technical Sciences*, Vol. 56, No. 4, pp. 319–324.

BUSŁOWICZ M. and Ruszewski A. (2013), "Necessary and sufficient conditions for stability of fractional discrete-time linear state-space systems", *Bulletin of the Polish Academy of Sciences: Technical Sciences*, Vol. 61, No. 4, pp. 779–786.

CATTANI C., Srivastava H. M. and Yang X.-J. (2015), *Fractional Dynamics*, Walter de Gruyter KG, Berlin, Germany.

CHEN W., Tang Y. and Karniadakis G. E. (2014), "Numerical methods for fractional partial differential equations with Riesz space fractional derivatives", *Journal of Computational Physics*, Vol. 258, pp. 601–615.

COBELLI C. and Foster D. (1998), "Compartmental models: theory and practice using the SAAM II software system", *Mathematical Modeling in Experimental Nutrition*, *Adv Exp Med Biol*, Vol. 445, pp. 79–101.

DIETHELM K. (2010), *The analysis of fractional differential equations: An application-oriented exposition using differential operators of Caputo type*, Springer, Berlin, Germany.

DORČÁK Ľ., Valsa J., Gonzalez E., Terpák J., Petráš I. and Pivka L. (2013), "Analogue Realization of Fractional-Order Dynamical Systems", *Entropy*, Vol. 15, No. 10, pp. 4199–4214.

DZİELİŃSKI A. and Sierociuk D. (2008), "Stability of discrete fractional order state-space systems", *Journal of Vibration and Control*, Vol. 14, No. 9–10, pp. 1543–1556.

EL-SAYED A. M. A. and Alsaedi A. (2014), "Dynamics of fractional-order predator-prey models with functional responses", *Advances in Difference Equations*, pp. 1–13.

GAO X.-L., Zhang H.-L., Wang Y.-L. and Li Z.-Y. (2024), "Research on Pattern Dynamics Behavior of a Fractional Vegetation-Water Model in Arid Flat Environment", *Fractal and Fractional*, Vol. 8, Issue 5, pp.264.

GORENFLO R., Mainardi F., Moretti D. and Paradisi P. (2002), "Discrete random walk models for space–time fractional diffusion", *Chemical Physics*, Vol. 284, No. 1–2, pp. 521–541.

HARKO T., Lobo F. S. and Mak M. K. (2014), "Exact analytical solutions of the Susceptible-Infected-Recovered (SIR) epidemic model and of the SIR model with equal death and birth rates", *Applied Mathematics and Computation*, Vol. 236, pp. 184–194.

HATTAF K. and Yousfi N. (2013), "A fractional order model for predicting future behavior of an infected prey population in a predator-prey system", *Nonlinear Analysis: Real World Applications*, Vol. 14, No. 1, pp. 180–193.

INOUE T. (2021), *The Advanced Theory of Fractional Calculus*, 3rd ed., Academic Research Publication, New York, NY, USA.

KEXUE D. and Ding J. (2013), "Fractional-order predator-prey models with Holling type II functional response", *Computational and Mathematical Methods in Medicine*, pp. 1–7.

KHAN A., Bai X., Ilyas M., Rauf A., Xie W., Yan P. and Zhang B. (2022), "Design and Application of an Interval Estimator for Nonlinear Discrete-Time SEIR Epidemic Models", *Fractal and Fractional*, Vol. 6, pp. 213.

KHAN M. (2022), "Interval Estimator for a Fourth-Order Nonlinear Susceptible–Exposed–Infected–Recovered (SEIR) Model with Disturbances and Noisy Data", *Journal of Biological Systems*, Vol. 58, No. 2, pp. 120–135.

KİLBAS A. A., Srivastava H. M. and Trujillo J. J. (2006), *Theory and applications of fractional differential equations*, Elsevier Science Limited, Amsterdam, Netherlands.

LI Y., Chen Y. and Podlubny I. (2010), "Stability of fractional-order nonlinear dynamic systems: Lyapunov direct method and generalized Mittag-Leffler stability", *Computers & Mathematics with Applications*, Vol. 59, No. 5, pp. 1810–1821.

MAGIN R. L. (2006), *Fractional calculus in bioengineering*, Begell House Publishers, New York, USA.

MAKHLOUF A. (2022), "Finite-Time Stability in Neutral Fractional-Order Systems with Time Delays", *Journal of Fractional Calculus*, Vol. 45, No. 3, pp. 200–210.

MATIGNON D. (1998), "Stability properties for generalized fractional differential systems", *ESAIM Proceedings*, Vol. 5, pp. 145–158.

MENDIOLA-FUENTES J. and Melchor-Aguilar D. (2018), "Modification of Mikhailov stability criterion for fractional commensurate order systems", *Journal of the Franklin Institute*, Vol. 355, pp. 2779–2790.

MERLIN S. D. (1949), *The Theory of Fluctuations in Contemporary Economic Thought*, Columbia University Press, New York, USA.

METZLER R. and Klafter J. (2000), "The random walk's guide to anomalous diffusion: A fractional dynamics approach", *Physics Reports*, Vol. 339, No. 1, pp. 1–77.

MONJE C. A. (2010), *Fractional-Order Systems and Controls: Fundamentals and Applications*, Springer, London, UK.

MOZYRSKA D. and Wyrwas M. (2018), "Stability of linear systems with Caputo fractional-variable-order difference operator of convolution type", *2018 41st International Conference on Telecommunications and Signal Processing (TSP)*, pp. 1–4, Athens, Greece.

MURESAN C. (2022), "Review of Auto-Tuning Approaches for Fractional-Order PID Controllers", *Journal of Control Engineering and Applications*, Vol. 32, No. 4, pp. 320–330.

MURESAN C. I., Birs I., Ionescu C., Dulf E. H. and De Keyser R. (2022), "A Review of Recent Developments in Autotuning Methods for Fractional-Order Controllers", *Fractal and Fractional*, Vol. 6, pp. 37.

N. GOKGOZ (2024), "Solution of fractional order sird model with adomian decomposition", *In*, *Recent Developments in Mathematics*, ch. 7, pp. 73–80, PEGEM Yayınevi, Ankara, Turkey.

N. GÖKGÖZ (2025), "An investigation of fractional-order respiratory system dynamics", *Cankaya University Journal of Science and Engineering*, Vol. 22, No. 1, pp. 33–41.

OLDHAM K. B. and Spanier J. (1974), *The fractional calculus: Theory and applications of differentiation and integration to arbitrary order*, Academic Press, New York, USA.

ORTIGUEIRA M. D. (2006), *Fractional calculus for scientists and engineers*, Springer, Berlin, Germany.

OSTALCZYK P. (2016), *Discrete Fractional Calculus: Applications in Control and Image Processing*, World Scientific, Singapore.

PETRÁŠ I. (2009), "Stability of fractional-order systems with rational orders: a survey", *Fractional Calculus and Applied Analysis*, Vol. 12, No. 3, pp. 269–298.

PODLUBNY I. (1999), *Fractional differential equations: An introduction to fractional derivatives, fractional differential equations, to methods of their solution and some of their applications*, Academic Press, San Diego, USA.

RAUH A. (2022), "Exponential Enclosures for the Verified Simulation of Fractional-Order Differential Equations", *Fractal and Fractional*, Vol. 6, pp. 567.

SINGH H., Srivastava H. M. and Nieto J. J. (2022), *Handbook of Fractional Calculus for Engineering and Science*, Chapman and Hall/CRC, Boca Raton, FL, USA.

STANISŁAWSKI R., Rydel M. and Latawiec K. J. (2018), "New stability tests for discretized fractional-order systems using the Al-Alaoui and Tustin operators", *Complexity*, 2018, Article ID 2036809, pp. 1–9.

SUN H., Zhang Y., Chen W. and Chen Y. Q. (2011), "A revised definition of the fractional derivative", *Nonlinear Dynamics*, Vol. 63, No. 3, pp. 365–372.

TARASOV V. E. (2011), "No violation of the Leibniz rule. No fractional derivative of a constant function", *Communications in Nonlinear Science and Numerical Simulation*, Vol. 16, No. 3, pp. 154–160.

TAVAZOEI M. and Asemani M. H. (2020), "On robust stability of incommensurate fractional-order systems", *Communications in Nonlinear Science and Numerical Simulation*, Vol. 90, pp. 105344.

THİRRİNG W. (2013), *Classical mathematical physics: dynamical systems and field theories*, Springer Science & Business Media, Berlin, Germany.

WU Z., Zhang X., Wang J. and Zeng X. (2023), "Applications of Fractional Differentiation Matrices in Solving Caputo Fractional Differential Equations", *Fractal and Fractional*, Vol. 6, pp. 1–20.

WYRWAS M., Mozyrska D. and Girejko E. (2013), "Stability of discrete fractional-order nonlinear systems with the Nabla Caputo difference", *IFAC Proceedings Volumes*, Vol. 46, No. 1, pp. 167–171.

YANG W., Zhang D., Peng L., Zhuge C. and Hong L. (2020), "Rational evaluation of various epidemic models based on the COVID-19 data of China", *Journal of Mathematical Modelling*, Vol. 10, pp. 1–15.

ZHANG H., Huang J. and He S. (2022), "Fractional-Order Interval Observer for Multiagent Nonlinear Systems", *Fractal and Fractional*, Vol. 6, pp. 355.

ZHAO T. and Chi Y. (2021), "Multiweighted-Type Fractional Fourier Transform: Unitarity", *Fractal and Fractional*, Vol. 5, pp. 205.

APPENDICES

APPENDIX 1:

```
function SEIQRV_Final_WithGamma
% SEIQRV
% ------------------------------------------------------------------------
% This script implements an advanced version of the SEIQRV model simulation:
%
% 1) 2D plots for multiple alpha values with key statistics printed (max values
%    for each compartment).
% 2) 3D plots showing how the solution changes with alpha.
% 3) A comparison plot between SIR, SEIR, SIS, Carrier, and SEIQRV models (focusing on I).
% 4) Printing R0 values and coupling points in a comparison table.
% 5) Local stability analysis using the Jacobian at the Disease-Free Equilibrium (DFE).
% 6) Determining if the SEIQRV system is in a Disease-Free Equilibrium or Endemic
%    state (based on R0).
% 7) Demonstrating the effect of changing gamma1 (vaccination rate) on V(t), R(t), and Q(t)
%    with separate subplots.
% 8) Creating a heatmap: maximum infected (I_max) vs. gamma1 and alpha1.
% 9) Bifurcation diagram: plotting the equilibrium value of I versus gamma1.
% ------------------------------------------------------------------------


clc; clear; close all;
```

```
%% == 1) DEFINE SEIQRV PARAMETERS & INITIAL CONDITIONS ===
% Model parameters:
params.alpha1 = 0.5;     % Transmission rate from Exposed (E) to Susceptible (S)
params.alpha2 = 0.1;  % Interaction coefficient between E and Vaccinated (V)
params.beta1  = 0.2;   % Rate at which S goes to Q (quarantine)
params.beta2  = 0.3;   % Rate at which E goes to Q
params.r1     = 0.25;  % Rate at which E goes to I (infected)
params.r2     = 0.15;  % Rate at which Q goes to I
params.sigma1 = 0.1;   % Recovery rate from S (or vaccination effect)
params.sigma2 = 0.2;   % Recovery rate from Q
params.sigma3 = 0.3;   % Recovery rate from I
params.gamma1 = 0.4;   % Vaccination rate
params.gamma2 = 0.05;  % Waning immunity rate
params.a      = 0.01;  % Natural death rate
params.Lambda = 0.1;   % Recruitment rate (new individuals entering the population)
params.N      = 1000;  % Total population
% Initial conditions: [S, E, I, Q, R, V]
S0 = 0.9 * params.N;
E0 = 0.05 * params.N;
I0 = 0.03 * params.N;
Q0 = 0.01 * params.N;
R0_ = 0.01 * params.N;
V0 = 0;
y0 = [S0; E0; I0; Q0; R0_; V0];
% Time settings:
tspan = [0 100];  % Simulation from 0 to 100 days
h = 0.1;          % Time step for the generalized Euler method
% Define multiple alpha values for simulation (e.g., [1.0, 0.9, 0.8])
alpha_values = [1.0, 0.9, 0.8];
```

```
compartments = {'S','E','I','Q','R','V'};
%% == 2) 2D PLOTS FOR SEIQRV AT MULTIPLE ALPHA & PRINT STATISTICS ==
figure('Name','SEIQRV - Multiple Alpha (2D)','NumberTitle','off');
numAlpha = length(alpha_values);

% Create a table to store max values for each compartment
statTable = cell(numAlpha+1, 7);
statTable(1,:) = {'alpha','max(S)','max(E)','max(I)','max(Q)','max(R)','max(V)'};
for idx = 1:numAlpha
    alpha_current = alpha_values(idx);
    [tSol, ySol] = gen_euler_fractional(@seiqrv_model, tspan, y0, params, alpha_current, h);
    % Plot each compartment in a subplot row
    subplot(numAlpha,1,idx);
    hold on;
    for cID = 1:6
        plot(tSol, ySol(:,cID), 'LineWidth',1.5, 'DisplayName', compartments{cID});
    end
    hold off; grid on;
    xlabel('Time (days)'); ylabel('Population');
    title(sprintf('SEIQRV with alpha = %.2f', alpha_current));
    legend('show','Location','best');
    % Compute maximum values for each compartment
    maxS = max(ySol(:,1));
    maxE = max(ySol(:,2));
    maxI = max(ySol(:,3));
    maxQ = max(ySol(:,4));
    maxR = max(ySol(:,5));
    maxV = max(ySol(:,6));
    statTable{idx+1,1} = alpha_current;
```

```
            statTable{idx+1,2} = maxS;
            statTable{idx+1,3} = maxE;
            statTable{idx+1,4} = maxI;
            statTable{idx+1,5} = maxQ;
            statTable{idx+1,6} = maxR;
            statTable{idx+1,7} = maxV;
            % Print a brief summary for this graph
            fprintf('\nGraph: "SEIQRV with alpha = %.2f"\n', alpha_current);
            fprintf('Max(S) = %.2f, Max(E) = %.2f, Max(I) = %.2f, Max(Q) = %.2f,
Max(R) = %.2f, Max(V) = %.2f\n', ...
                maxS, maxE, maxI, maxQ, maxR, maxV);
        end
        fprintf('\n== SEIQRV Max-Compartment Statistics for Different Alpha
==\n');
        disp(statTable);
        %% = 3) DETERMINE IF SEIQRV IS DFE OR ENDEMIC (BASED ON
R0) =
        % Calculate R0 for SEIQRV using the Next-Generation Matrix method:
        % R0 = alpha1 / (a + beta2 + r1)
        R0_SEIQRV = params.alpha1 / (params.a + params.beta2 + params.r1);
        fprintf('\nSEIQRV Basic Reproduction Number R0 = %.4f\n',
R0_SEIQRV);
        if R0_SEIQRV < 1
            fprintf('=> R0 < 1, thus the system tends to a Disease-Free Equilibrium
(DFE)\n');
        else
            fprintf('=> R0 > 1, thus the system tends to an Endemic Equilibrium\n');
        end
        %% ========== 4) COMPARE SIR, SEIR, SIS, CARRIER, &
SEIQRV (INFECTED) ============
        % Use alpha = 1 for SEIQRV comparison
        alpha_compare = 1.0;
```

```
[t_cmp, y_cmp] = gen_euler_fractional(@seiqrv_model, tspan, y0, params, alpha_compare, h);
I_SEIQRV = y_cmp(:,3);
% SIR model
beta_sir = 0.3; gamma_sir = 0.1;
y0_sir = [S0; I0; R0_];
[t_sir, sol_sir] = ode45(@(t,y) sir_model(t,y,beta_sir,gamma_sir), tspan, y0_sir);
I_SIR = sol_sir(:,2);
% SEIR model
beta_seir = 0.3; a_seir = 0.1; gamma_seir = 0.1;
y0_seir = [S0; E0; I0; R0_];
[t_seir, sol_seir] = ode45(@(t,y) seir_model(t,y,beta_seir,a_seir,gamma_seir), tspan, y0_seir);
I_SEIR = sol_seir(:,3);
% SIS model
beta_sis = 0.3; gamma_sis = 0.1;
y0_sis = [I0];
[t_sis, sol_sis] = ode45(@(t,y) sis_model(t,y,beta_sis,gamma_sis,params.N), tspan, y0_sis);
I_SIS = sol_sis(:,1);
% Carrier model
beta_car = 0.2; eta_car = 0.05; alpha_car = 0.1; gamma_car = 0.1; eps_car = 0.05;
y0_carrier = [S0; I0; 0; R0_];
[t_car, sol_car] = ode45(@(t,y) carrier_model(t,y,beta_car,eta_car,alpha_car,gamma_car,eps_car), tspan, y0_carrier);
I_Carrier = sol_car(:,2);
% Plot the comparison for the Infected compartment
figure('Name','Model Comparison (Infected)','NumberTitle','off');
plot(t_sir, I_SIR, 'b', 'LineWidth',2, 'DisplayName','SIR (I)'); hold on;
plot(t_seir, I_SEIR, 'r', 'LineWidth',2, 'DisplayName','SEIR (I)');
```

```
plot(t_sis, I_SIS, 'g', 'LineWidth',2, 'DisplayName','SIS (I)');
plot(t_car, I_Carrier, 'm', 'LineWidth',2, 'DisplayName','Carrier (I)');
plot(t_cmp, I_SEIQRV, 'k', 'LineWidth',2, 'DisplayName','SEIQRV (I)');
  hold off; grid on;
  xlabel('Time (days)'); ylabel('Infected');
  title('Comparative Analysis of Infected Dynamics');
  legend('show','Location','best');
  %% == 5) PRINT R0 & COUPLING POINTS FOR ALL MODELS IN A TABLE ==
  % Calculate R0 for each model:
  R0_SIR = (beta_sir * params.N) / gamma_sir;
  R0_SEIR = (beta_seir * params.N) / gamma_seir;
  R0_SIS  = beta_sis / gamma_sis;
  R0_Carrier = (beta_car * params.N + eta_car * params.N) / gamma_car;
  % Define coupling points (textual summary)
  c_SIR     = '(-beta*S*I)';
  c_SEIR    = '(-beta*S*I)';
  c_SIS     = '(beta*I*(N-I))';
  c_Carrier = '(-beta*S*I - eta*C*S)';
  c_SEIQRV  = '(alpha1*S*E/N, beta1*S, gamma1*S, ...)';
  compTable = {
    'Model', 'R0',        'Coupling Points';
    'SIR',   R0_SIR,      c_SIR;
    'SEIR',  R0_SEIR,     c_SEIR;
    'SIS',   R0_SIS,      c_SIS;
    'Carrier', R0_Carrier, c_Carrier;
    'SEIQRV', R0_SEIQRV,  c_SEIQRV;
  };
  fprintf('\n==== Comparison of Models: R0 & Coupling Points ====\n');
  disp(compTable);
  %% = 6) LYAPUNOV (LOCAL STABILITY) CHECK AT DFE (SEIQRV) ==
  % Calculate the Jacobian at the Disease-Free Equilibrium (DFE)
```

```
S_eq = params.N; E_eq = 0; I_eq = 0; Q_eq = 0; R_eq = 0;
% From dV/dt=0, assume V_eq = (gamma1*N)/(gamma2+a)
V_eq = (params.gamma1 * params.N) / (params.gamma2 + params.a);
x_eq = [S_eq; E_eq; I_eq; Q_eq; R_eq; V_eq];
J = Jacobian_SEIQRV(x_eq, params);
eigenVals = eig(J);
fprintf('\n==== SEIQRV: Eigenvalues at DFE ====\n');
disp(eigenVals);
stableLocal = all(real(eigenVals) < 0);
if stableLocal
   fprintf('=> DFE is locally asymptotically stable (all eigenvalues negative)\n');
else
   fprintf('=> DFE is unstable (some eigenvalue has positive real part)\n');
end
% Note: Global stability analysis would involve evaluating a Lyapunov function.
%% ==== 7) 3D PLOT: INFECTED vs TIME vs ALPHA ====
alphaFine = linspace(1, 0.8, 10);
tSteps = 0:h:100;
nA = length(alphaFine);
nT = length(tSteps);
I_matrix = zeros(nT, nA);
for aInd = 1:nA
   alphaVal = alphaFine(aInd);
   [~, yTemp] = gen_euler_fractional(@seiqrv_model, tspan, y0, params, alphaVal, h);
   I_matrix(:, aInd) = yTemp(:,3);
end
figure('Name','3D Plot: I(t, alpha)','NumberTitle','off');
[Agrid, Tgrid] = meshgrid(alphaFine, tSteps);
surf(Tgrid, Agrid, I_matrix); shading interp;
xlabel('Time (days)'); ylabel('Alpha'); zlabel('Infected (I)');
```

```
title('SEIQRV: 3D Plot of I(t, alpha)');
%% ====== 8) 3D SURFACES FOR EACH COMPARTMENT ======
alpha3D = linspace(1, 0.8, 6);
[Smat, Emat, Imat, Qmat, Rmat, Vmat, tBase] = do3DDataSEIQRV(y0, params, alpha3D, h);
figure('Name','3D Surfaces for Each Compartment','NumberTitle','off');
c3d = {'S', 'E', 'I', 'Q', 'R', 'V'};
for iC = 1:6
   subplot(2,3, iC);
   switch iC
      case 1, Z = Smat;
      case 2, Z = Emat;
      case 3, Z = Imat;
      case 4, Z = Qmat;
      case 5, Z = Rmat;
      case 6, Z = Vmat;
   end
   [Agrid, Tgrid] = meshgrid(alpha3D, tBase);
   surf(Tgrid, Agrid, Z); shading interp;
   xlabel('Time (days)'); ylabel('Alpha'); zlabel(c3d{iC});
   title(['3D - ', c3d{iC}]);
end
sgtitle('SEIQRV: 3D Surfaces vs. Alpha and Time');
%% ====== 9) EFFECT OF CHANGING gamma1 ON (V, R, Q) ======
gamma1_list = [0.1, 0.3, 0.5, 0.7];
alpha_main = 1.0;  % Use alpha = 1.0 for these runs
figure('Name','Effect of Changing gamma1 on (V, R, Q)','NumberTitle','off');
subplot(1,3,1); hold on; grid on; title('V(t)');
xlabel('Time (days)'); ylabel('Vaccinated');
subplot(1,3,2); hold on; grid on; title('R(t)');
```

```
            xlabel('Time (days)'); ylabel('Recovered');
            subplot(1,3,3); hold on; grid on; title('Q(t)');
            xlabel('Time (days)'); ylabel('Quarantined');
            gammaStats = cell(length(gamma1_list)+1, 4);
            gammaStats(1,:) = {'gamma1','max(V)','max(R)','max(Q)'};
            for iG = 1:length(gamma1_list)
                gVal = gamma1_list(iG);
                oldGamma1 = params.gamma1;
                params.gamma1 = gVal;
                [t_g, y_g] = gen_euler_fractional(@seiqrv_model, tspan, y0, params,
alpha_main, h);
                Vtemp = y_g(:,6);
                Rtemp = y_g(:,5);
                Qtemp = y_g(:,4);
                subplot(1,3,1); plot(t_g, Vtemp, 'LineWidth',2, 'DisplayName',
['\gamma1=', num2str(gVal)]);
                subplot(1,3,2); plot(t_g, Rtemp, 'LineWidth',2, 'DisplayName',
['\gamma1=', num2str(gVal)]);
                subplot(1,3,3); plot(t_g, Qtemp, 'LineWidth',2, 'DisplayName',
['\gamma1=', num2str(gVal)]);
                gammaStats{iG+1,1} = gVal;
                gammaStats{iG+1,2} = max(Vtemp);
                gammaStats{iG+1,3} = max(Rtemp);
                gammaStats{iG+1,4} = max(Qtemp);
                params.gamma1 = oldGamma1;
            end
            subplot(1,3,1); legend('show','Location','best');
            subplot(1,3,2); legend('show','Location','best');
            subplot(1,3,3); legend('show','Location','best');
            fprintf('\n==== Effect of Changing gamma1 on V, R, Q (alpha = %.2f)
====\n', alpha_main);
            disp(gammaStats);
```

```
%% === 10) HEATMAP: MAX INFECTED (I_max) VS gamma1 & alpha1 ===
% Vary both gamma1 and alpha1 and compute the maximum value of I for each combination.
gamma1_range = linspace(0.1, 0.7, 10);
alpha1_range = linspace(0.3, 0.7, 10); % adjust as needed
Imax_matrix = zeros(length(gamma1_range), length(alpha1_range));
for i = 1:length(gamma1_range)
   for j = 1:length(alpha1_range)
      tempParams = params;
      tempParams.gamma1 = gamma1_range(i);
      tempParams.alpha1 = alpha1_range(j);
      [~, y_temp] = gen_euler_fractional(@seiqrv_model, tspan, y0, tempParams, 1.0, h);
      Imax_matrix(i,j) = max(y_temp(:,3));
   end
end
figure('Name','Heatmap: Max I vs gamma1 & alpha1','NumberTitle','off');
imagesc(alpha1_range, gamma1_range, Imax_matrix);
colorbar;
xlabel('alpha1'); ylabel('gamma1');
title('Heatmap of Max(I) vs gamma1 and alpha1');
% Explanation: Regions with high I indicate sensitivity to changes in vaccination and transmission.
%% ===== 11) BIFURCATION DIAGRAM: Equilibrium I vs gamma1 =====
% Vary gamma1 and record the equilibrium value of I (last value at t = 100)
gamma1_vals = linspace(0.1, 0.7, 20);
I_eq_vals = zeros(length(gamma1_vals), 1);
for k = 1:length(gamma1_vals)
   tempParams = params;
   tempParams.gamma1 = gamma1_vals(k);
```

```
        [~, y_eq] = gen_euler_fractional(@seiqrv_model, tspan, y0, tempParams, 1.0, h);
        I_eq_vals(k) = y_eq(end,3);
    end
    figure('Name','Bifurcation Diagram: Equilibrium I vs gamma1','NumberTitle','off');
    plot(gamma1_vals, I_eq_vals, 'k-o', 'LineWidth',2);
    xlabel('gamma1'); ylabel('Equilibrium I');
    title('Bifurcation Diagram: Equilibrium I vs gamma1');
    % Explanation: This diagram shows how the equilibrium level of I changes with gamma1.
    % For lower gamma1, the system may be endemic; as gamma1 increases, I may drop to DFE levels.
    fprintf('\n--- End of SEIQRV_Final_WithGamma script. All requested data and plots generated. ---\n');
end
%% ======================
%                SEIQRV MODEL EQUATIONS
%%======================
function dydt = seiqrv_model(~, y, params)
    % SEIQRV model equations: y = [S, E, I, Q, R, V]
    S = y(1); E = y(2); I = y(3); Q = y(4); R = y(5); V = y(6);
    N_current = S + E + I + Q + R + V;
    dSdt = params.Lambda - (params.alpha1 * S * E / N_current) - params.beta1 * S - params.sigma1 * S - params.a * S;
    dEdt = (params.alpha1 * S * E / N_current) - params.r1 * E - params.beta2 * E - params.a * E + (params.alpha2 * E * V / N_current);
    dIdt = params.r1 * E + params.r2 * Q - params.sigma3 * I - params.a * I;
    dQdt = params.beta1 * S + params.beta2 * E - params.r2 * Q - params.sigma2 * Q - params.a * Q;
    dRdt = params.sigma1 * S + params.sigma2 * Q + params.sigma3 * I - params.a * R;
```

```
        dVdt = params.gamma1 * S - params.gamma2 * V - (params.alpha2 * E
* V / N_current) - params.a * V;
        dydt = [dSdt; dEdt; dIdt; dQdt; dRdt; dVdt];
    end
    %% ==================
    %       GENERALIZED EULER METHOD FOR FRACTIONAL-ORDER
ODEs
    %% ==================
    function [t, y] = gen_euler_fractional(funHandle, tspan, y0, params, alpha,
h)
        t0 = tspan(1); tf = tspan(2);
        t = (t0:h:tf)';
        n = length(t);
        m = length(y0);
        y = zeros(n, m);
        y(1,:) = y0';
        frac_coef = h^alpha / gamma(alpha+1);
        for i = 1:n-1
            f_now = funHandle(t(i), y(i,:)', params);
            y(i+1,:) = y(i,:) + frac_coef * f_now';
        end
    end
    %% ========================
    %    JACOBIAN FOR SEIQRV AT AN EQUILIBRIUM POINT (LOCAL
STABILITY)
    %% ========================
    function J = Jacobian_SEIQRV(x_eq, params)
        % x_eq = [S; E; I; Q; R; V]
        S = x_eq(1); E = x_eq(2); I = x_eq(3);
        Q = x_eq(4); R = x_eq(5); V = x_eq(6);
        N = S + E + I + Q + R + V;
        % Partial derivatives for dS/dt
```

```
        dF1dS = - (params.alpha1 * E / N) - params.beta1 - params.sigma1 -
params.a;
        dF1dE = - (params.alpha1 * S / N);
        dF1dI = 0; dF1dQ = 0; dF1dR = 0; dF1dV = 0;
        % Partial derivatives for dE/dt
        dF2dS = (params.alpha1 * E / N);
        dF2dE = (params.alpha1 * S / N) - params.r1 - params.beta2 - params.a +
(params.alpha2 * V / N);
        dF2dV = (params.alpha2 * E / N);
        dF2dI = 0; dF2dQ = 0; dF2dR = 0;
        % Partial derivatives for dI/dt
        dF3dE = params.r1;
        dF3dQ = params.r2;
        dF3dI = - params.sigma3 - params.a;
        dF3dS = 0; dF3dR = 0; dF3dV = 0;
        % Partial derivatives for dQ/dt
        dF4dS = params.beta1;
        dF4dE = params.beta2;
        dF4dQ = - params.r2 - params.sigma2 - params.a;
        dF4dI = 0; dF4dR = 0; dF4dV = 0;
        % Partial derivatives for dR/dt
        dF5dS = params.sigma1;
        dF5dQ = params.sigma2;
        dF5dI = params.sigma3;
        dF5dR = - params.a;
        dF5dE = 0; dF5dV = 0;
        % Partial derivatives for dV/dt
        dF6dS = params.gamma1;
        dF6dV = - params.gamma2 - params.a - (params.alpha2 * E / N);
        dF6dE = - (params.alpha2 * V / N);
        dF6dI = 0; dF6dQ = 0; dF6dR = 0;
        J = [ dF1dS, dF1dE, dF1dI, dF1dQ, dF1dR, dF1dV;
            dF2dS, dF2dE, dF2dI, 0,      0,      dF2dV;
```

```
            0,      dF3dE, dF3dI, dF3dQ, 0,      0;
            dF4dS, dF4dE, dF4dI, dF4dQ, 0,      0;
            dF5dS, 0,      dF5dI, dF5dQ, dF5dR, 0;
            dF6dS, dF6dE, 0,      0,      0,      dF6dV ];
    end
    %% ====================================
    %  HELPER FUNCTION: BUILD 3D DATA FOR (S,E,I,Q,R,V) VS TIME VS ALPHA
    %% ====================================
    function [Smat, Emat, Imat, Qmat, Rmat, Vmat, tBase] = do3DDataSEIQRV(y0, params, alphaVec, h)
        tspan = [0 100];
        tBase = (0:h:100)';
        nT = length(tBase);
        nA = length(alphaVec);
        Smat = zeros(nT, nA); Emat = zeros(nT, nA);
        Imat = zeros(nT, nA); Qmat = zeros(nT, nA);
        Rmat = zeros(nT, nA); Vmat = zeros(nT, nA);
        for iA = 1:nA
            alphaVal = alphaVec(iA);
            [~, ySol] = gen_euler_fractional(@seiqrv_model, tspan, y0, params, alphaVal, h);
            Smat(:, iA) = ySol(:,1);
            Emat(:, iA) = ySol(:,2);
            Imat(:, iA) = ySol(:,3);
            Qmat(:, iA) = ySol(:,4);
            Rmat(:, iA) = ySol(:,5);
            Vmat(:, iA) = ySol(:,6);
        end
    end
    %% ======================
    %              ANCILLARY MODELS (SIR, SEIR, SIS, CARRIER)
    %% ======================
```

```
function dydt = sir_model(~, y, beta, gamma)
    % SIR model equations: y = [S; I; R]
    S = y(1); I = y(2);
    dSdt = -beta * S * I;
    dIdt = beta * S * I - gamma * I;
    dRdt = gamma * I;
    dydt = [dSdt; dIdt; dRdt];
end
function dydt = seir_model(~, y, beta, a_, gamma)
    % SEIR model equations: y = [S; E; I; R]
    S = y(1); E = y(2); I = y(3);
    dSdt = -beta * S * I;
    dEdt = beta * S * I - a_ * E;
    dIdt = a_ * E - gamma * I;
    dRdt = gamma * I;
    dydt = [dSdt; dEdt; dIdt; dRdt];
end
function dydt = sis_model(~, y, beta, gamma, N)
    % SIS model: y = [I], with S = N - I
    I = y(1);
    dIdt = beta * I * (N - I) - gamma * I;
    dydt = dIdt;
end
function dydt = carrier_model(~, y, beta, eta, alpha_c, gamma, eps_c)
    % Carrier model equations: y = [S; I; C; R]
    S = y(1); I = y(2); C = y(3);
    dSdt = -beta * S * I - eta * C * S;
    dIdt = beta * S * I + eta * C * S - alpha_c * I - gamma * I + eps_c * C;
    dCdt = alpha_c * I - eps_c * C;
    dRdt = gamma * I;
    dydt = [dSdt; dIdt; dCdt; dRdt];
end
```